高屏溪斜張橋監測系統-結構狀況長期監測

Monitoring system of Kao Ping Hsi Cable-Stayed Bridge - Long term structural performance monitoring

South Region Engineering Office, Taiwan Area National Freeway Bureau, Ministry of Transportation and Communications

Contents

Abstract

A bridge crossing Kao Ping Hsi was built in 1999 at Yen Chao Chiu Ju section of Freeway 3, spanning 2,617m and 34.5m wide. 3 traffic lanes were established at each of southbound and northbound directions. The 150m-long main span over the river was designed to be a non-symmetric single-tower complex cable-stayed bridge, which is named “Kao Ping Hsi Cable-Stayed Bridge” or the Bridge as follows. The main span is steel structure with a length of 330m. 15 pairs of cable (30 cables) were used to suspend the main girders at each of the main and ramp spans, totaling 60 steel cables along the entire Bridge arranged in a radiating fashion. Being the longest cable-stay bridge in Taiwan, the Bridge is a slender, light-weight and flexible design. Therefore, the monitoring of winds to which the Bridge is sensitive is no less important than the monitoring of seismic activities. The monitoring system installed on the Bridge during the construction stage was designed primarily for the monitoring of construction and the stresses in the structural materials. This system served as the best source of information and data regarding the

health of the Bridge, thus helping keep the Bridge safe while the construction was at full swing. At present, the Bridge has been bearing the loads of traffic for more than a decade. To ensure the safety of the Bridge, the Bureau has developed a bridge health monitoring system (BHMS) for the long-term monitoring of the overall structural safety over the entire operation stage in terms of seismic response, wind resisting response and cable vibration, as well as travel comfort. The BHMS will provide more alarm information for the study of bridge safety management and maintenance in relation to seismic activities, wind vibration and traffic.

1. Introduction

Cable-stayed bridge features a degree of aesthetics and the economic benefit of ultra-long spans. The design of cable-stayed bridge became fashionable thanks to the advancing of engineering technology (Yang and Chen, 1995[a]). Therefore, led by sea-crossing cable-stayed bridges in Japan and Denmark, the bridge engineering in the world has moved into a new era in the 21st century, an era of "strait-crossing bridge," for example, the Messina Bridge connecting Sicily and mainland Italy; the bridge over Bosporus Strait connecting Asia and Europe; the bridge over La Pérouse Strait between Japan and Russia and the one over Tatar Strait; and the bridges connecting the three island of Britain. China, of course, will not stay out of this "fashion" of building world-class bridges, as some sea-crossing bridges are now on design desk or being built, such as the bridges over the strait of Bohai sea, the mouth o Yangtze River and Zhujian River, Hangzhou Bay and Qiongzhou Strait. For example, the 1,088m main span of Sutong Bridge was connected in Sep 2007. If completed, this bridge will be longer than the Tatara Bridge in Japan, which is 890m long, and become the cable-stayed bridge in the world that has the longest span. In addition, located at southern France, the Millau Viaduct is nicknamed "the bridge in the cloud" by international bridge engineering society. It was a world phenomenon even when it was being built. The Millau Viaduct is the tallest cable-stayed bridge. Its tallest pier is 244.96m tall, and the elevation of the highest point on the bridge is 343m. The length is 2,460m from end to end, and the spans are 204m + 6@342m + 204m. The largest span of the cable-stayed section is 342m. These bridges are truly some of the greatest breakthroughs of world bridge engineering in the 21st

century.

With the completion of Kao Ping Hsi Cable-Stayed Bridge on Freeway 3 and the advancing bridge technology in Taiwan, there are an increasing number of cable-stayed bridges designed for river crossing, including the fishing pole cable-stayed bridge at Dazhi, Taipei, steel arch tower cable-stayed bridge and Chilu Bridge in Nantou, the cable-stayed bridge over the Erchong causeway in New Taipei City, Shehtzu Bridge and several curved cable-stayed bridges over Danshui River designed for pedestrian. These are the examples showing the improvement of bridge engineering in Taiwan and the footsteps to catch up with the rest of the world. On the other hand, with the fast development of cable-stayed bridges, there are still several concerns, such as the safety maintenance strategies after they are commissioned for traffic, whether there is a system for damage assessment, and whether bridge engineers are up for the upcoming challenge that we may neglect some problems that will result in failure of these engineering marvels under the pressure of not wanting to be left behind in this international engineering ranking of cable-stayed bridge (Yang and Chen, 1995[b]).

In addition, the stay cables are one of the most difficult components to maintain for the safety of bridge after it is open for traffic, as the slenderness ratio is large, and they are flexible, low in damping ratio and less resistant to bending. It is possible that the cable snaps under large cyclic flexural stress due to wind-induced motion, regular traffic or even ambient vibration, as shown in **Fig. 1.1** (Siegert and Brevet, 2006). The loosening seal of stay cables, damaged anchors, and tendon corrosion due to damaged protection sleeve at the root will undermine dramatically the life of cable-stayed bridge and even its safety. Also, normal loads such as traffic and wind are acting on the stay cables every minute of the bridge's life. The damaged cables may be replaced, but there is no guarantee that the same damage will not occur again. Stay cables are damaged due to vibration. Therefore, the changes in mechanical behavior of stay cables under normal traffic, occasional earthquakes or typhoons, fatigue accumulated over time, and loss of tensioning are some of the potential crises for cable-stayed bridges, and the key points of routine inspection and maintenance or long-term maintenance (Chen and Weng, 2007).

This report contains two major parts; the first is the introduction of in-situ vibration monitoring and measurement techniques that help obtain the basic characteristics of a bridge as the basis of comparison for the health monitoring needed for the BHMS; and the second is the introduction of how a complete BHMS is designed and installed as the basis of cable-stayed bridge characteristic changes monitoring and the assessment of bridge safety.

Figure 1.1 Rupture of stay cable due to fatigue (Siegert and Brevet 2006)

2. Description of Kao Ping Hsi Cable-Stayed Bridge

The Kao Ping Hsi Cable-Stayed Bridge is the main bridge that crosses over Kao Ping Hsi at Yen Chao Chiu Ju section of Freeway 3, as shown in **Fig. 2.1**. At 510m long, the Bridge is a non-symmetric structure combining large spans and a single tower, as shown in **Fig. 2.2**. The 330m main span is a steel structure, and the 180m side span is an PC structure. At 183.5m tall, the tower is an inverted-Y RC structure. The main span and side span are suspended with 14 sets of stay cables, 4 cables in the outermost set on each of the span and 2 in the rest of the sets, as shown in **Fig. 2.3**. In total, 60 steel cables support the entire bridge. **Fig. 2.3** shows that the cables closest to abutment A1 are B101 and B101A, while cable B114 is the one closet to tower P1 in the side span. F114 is the cable closet to tower P1 in the main span, whereas F101A and F101 are closet to pier P2. The stay cables of the bridge fan out in a single plane with double cable sets, as shown in **Fig. 2.3**.

Fig. 2.4 shows the cross section of the stay cable. The geometry of a stay cable is designed

into two categories according to the design requirements of Taiwan Area National Expressway Engineering Bureau (2002): one is the 15.2mmψ-ASTM A416-90a 270 low-relaxation steel strands and the other is 15.7mmψ-BS-5896 170 Class II low-relaxation steel strands. There are Type A and Type B cables; there are 46 Type A cables with the maximum of 91 steel stands, and 14 Type B cables with the maximum of 61 steel strands, in total 60 cables.

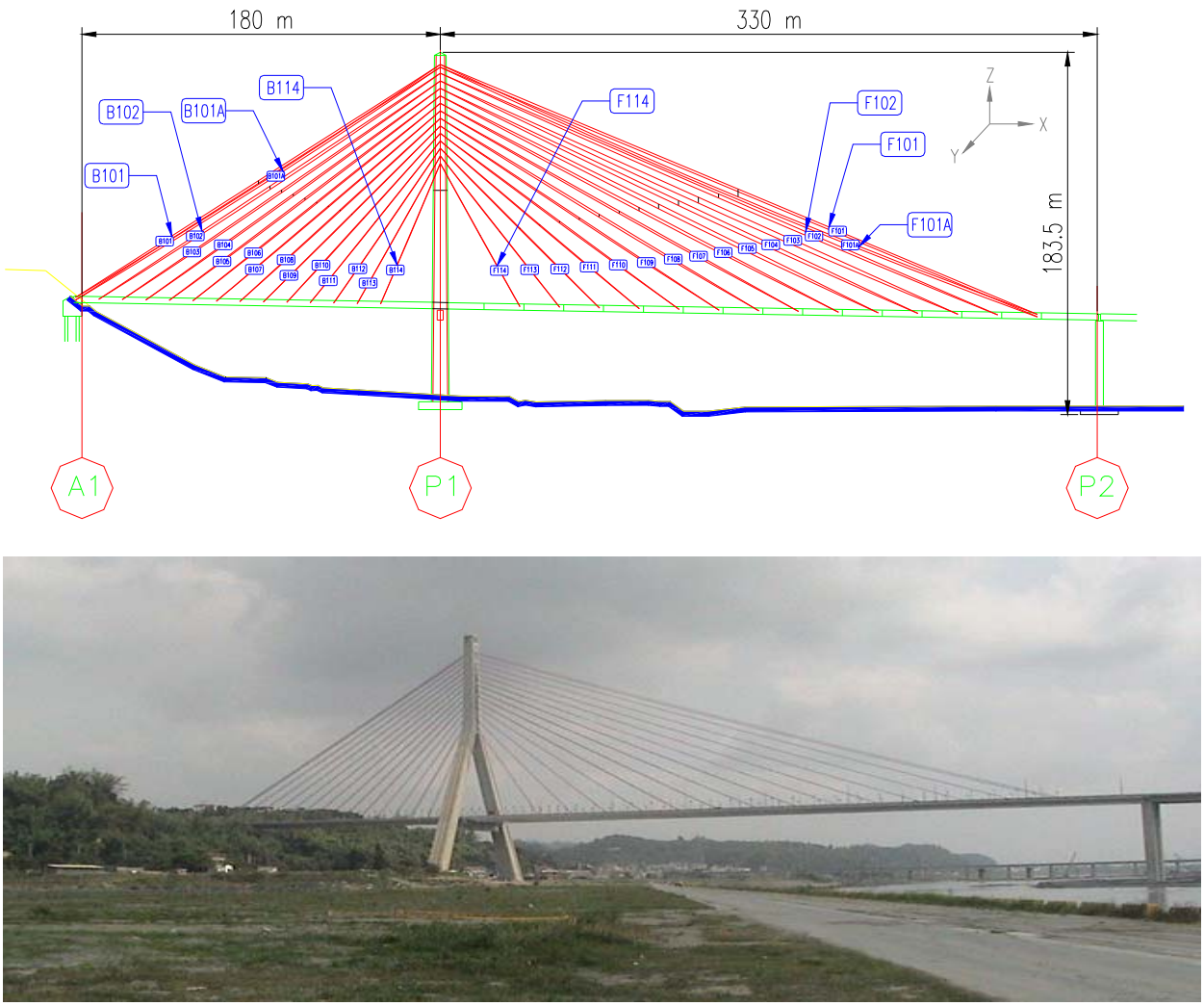

Figure 2.1 The Kao Ping Hsi Cable-Stayed Bridge

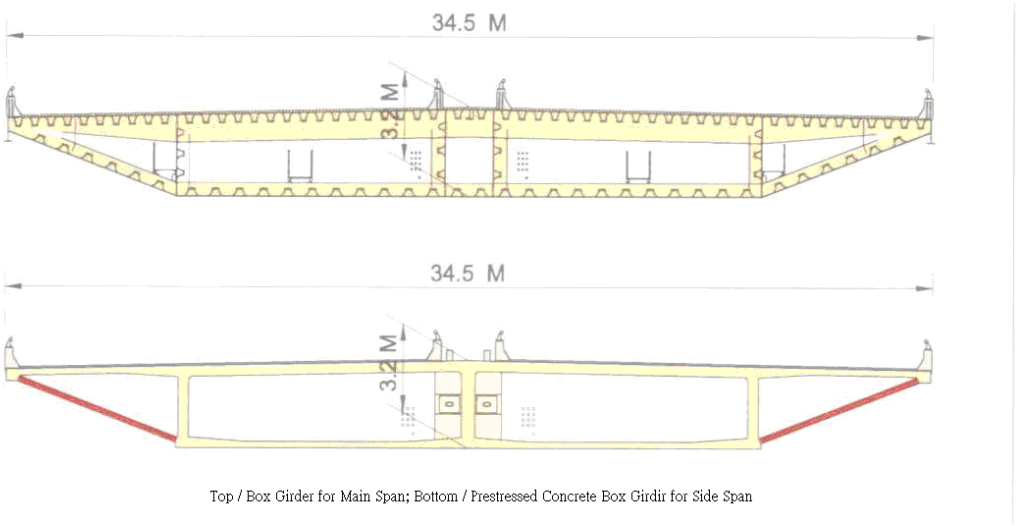

Figure 2.2 Cross Section of Kao Ping Hsi Cable-Stayed Bridge (Taiwan Area National Expressway Engineering Bureau, 2002)

Figure 2.3 Arrangement of Stay Cables in Pairs

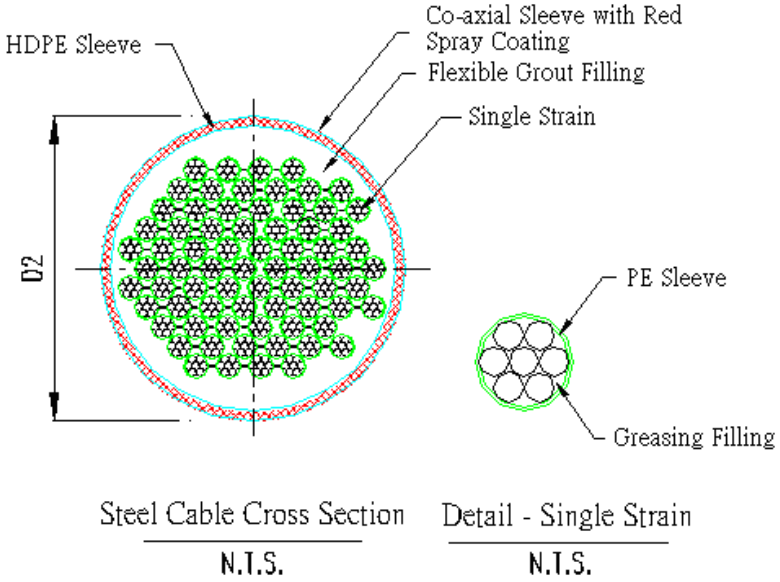

Figure 2.4 Cross Section of Stay Cable (Taiwan Area National Expressway Engineering Bureau, 2002)

3. Bridge Health Monitoring System

3.1 Design demands

The BHMS of the Bridge is established in two stages:

1. The focus of stage 1 is on the establishment of a complete monitoring system and the necessary inspection, testing and measurement of the entire bridge. The initial parameters of the bridge needed for the monitoring work are included in the "bridge management database for Kao Ping Hsi Cable-Stayed Bridge." Another key point is the collection of in-situ measurement data, including parameters related to seismic activities, traffic, winds and vibrations. Analysis and assessment are carried out to establish the necessary parameters needed for the monitoring of the Bridge's health and the development of monitoring criteria and alarm values.
2. The aim of stage 2 is to re-assess the monitoring alarm criteria. The client's demands are considered, while the control center network is brought in to provide the maintenance of the traffic safety and wind resistant performance of the Bridge and complete alarm information. The "bridge management database for Kao Ping Hsi Cable-Stayed Bridge" is established. In addition, the alarm information will help the establishment of bridge closing mechanism and the number of monitoring spots and items may be increased based on the demands of safety control and practical functions. The alarm values developed with more reliable array of monitoring concepts will be used as the basis of traffic control, the establishment of traffic control facilities and implementation of closing the bridge at time of danger. By doing all these, the action and purpose of monitoring the Bridge's safety will be embodied, and the goal of monitoring, control and safety will be achieved.

3.2 Monitoring and analysis demands

The development of monitoring items and the functions for the cable-stayed bridge monitoring system requires the analysis and investigation of the bridge's characteristics and current status as it

is. The monitoring instruments are placed at spots where are sensitive to damage. By studying the changes in characteristic parameters after the bridge is loaded, it is possible to determine the damage to the bridge. In addition, the Bridge is one on national freeway. An alarm can be issued only when the damage is determined very accurately when the Bridge is loaded. As a result, all the monitoring indicators must be collected and studied to reach the demand for multiple monitoring indicators and to arrive at the best judgment. The following are the preparation for the implementation of long-term monitoring and items of analysis for the Bridge, and the results will be introduced in the design of monitoring system. The monitoring and analysis demands are:

1. Vibration test and system identification: to establish a reasonable finite element analysis model for seismic and wind loading analysis.
2. Cable tensioning measurement and analysis: to establish the clear picture of the tensioning on all cables for the behavioral analysis of the wind and rain vibrations of the Bridge.
3. Aerodynamic stability analysis: to carry out the aerodynamic stability analysis of the entire Bridge.
4. Influence of traffic effects on bridge vibrations.

3.3 Planning of work items for the monitoring system

The monitoring system is designed based on in-situ tests and theoretical basis with the analysis on the test results available, inspection result and subsequent monitoring key points. As the Bridge is an important bridge on the national freeway, it is necessary to have a system capable of "multiple monitoring" to provide sufficient and reliable information for the judgment of closing the Bridge for possible risks and the safety of drivers, and to prevent possible mistakes of closing the Bridge depending on only a single monitoring value. Thus, the structure of subsequent monitoring system and items of monitoring are proposed as follows:

1. Monitoring of seismic activities and high winds

The new seismometers and anemometers/weathervanes are used to obtain the ground acceleration of an earthquake and the time-history of in-situ wind speed and direction, as well as

simple spectrum analysis. Combining the above and the establishment of recommended alarm values, the necessary real-time alarm function is developed.

2. Measurement of tower and main girder vibrations in event of earthquakes

Accelerometers located on the bridge tower and main girders are used to obtain the time-history of the acceleration and the simple spectrum analysis. GPS is used to measure the absolute displacement, and the frequency distribution is monitored constantly for the comparison with historic test or monitoring data. In the event of earthquake, in addition to examining and comparing the frequency distribution, the maximum displacements of tower and main girders are calculated using the time-history obtained in order to determine whether the primary structure is compromised.

3. Bridge deck displacement measurement

The absolute displacements are collected using the signals transmitted from the GPS-based displacement sensor located on main girders, and time-history is measured using speedometer. The displacement time-history is obtained through integral calculus and compared with the GPS data for more alarm parameters.

4. Measurement of tensioning changes in stay cables

(1) To evaluate the changes in each of the cables to determine if the tensioning capacity is still within a safe range;

(2) To monitor the vibration of cables in high winds to determine the stability of cables;

(3) To evaluate the effects or wind and rain to the stability of main girders and cables to determine the stability of cables in winds;

(4) To evaluate the vibration of cables in an earthquake; and

(5) To evaluate the vibrations due to normal traffic and parametric resonance.

5. Wind field characteristics measurement and typhoon monitoring

The Bridge is located at an open field. According to the “Wind design code for buildings and commentary” developed by Architecture and Building Research Institute, MOI, the site is a Category C site. To measure the actual wind filed, 3D ultrasonic anemometer is used and the

wind speed response frequency is determined to be 10Hz, which reflects correctly the wind speed disturbance characteristics.

6. Evaluation of driving safety under wind effects

The Bridge comes out of hills from west and extends eastwards into the flat Kao Ping Hsi valley at a 1.7% downward gradient to the east. The bridge deck is approximately 50m above the river. To the east of the Bridge is a somewhat featureless flatland, resulting in possible concerns regarding the driving safety, as high wind speeds are detected due to high-speed airflows that come to the Bridge from afar. The design and alarm functions of the monitoring system mentioned are evaluated for the driving safety on the Bridge. In addition, 3 solutions are proposed for the safety at potentially dangerous sections. The first is the static model, for which the high wind speed is dealt with using active and passive means, such as wind breaking installations, speed limits and warning signs for high winds, according to the sections where dangerously high wind speed occurs. The other is the dynamic model, for which wind speeds are constantly monitored at sections of clearly high winds. When the wind speed exceeds the upper limit, an alarm signal is generated and emergency response is initiated.

7. Remote transmission and monitoring

Thanks to the advanced Internet technology, ADSL access is very popular. This can be elaborated in 4 ways:

(1) Application: ADSL (Asymmetric Digital Subscriber Line) refers to the technology of adding an ATU-R (ADSL modem) on the existing telephone line. With ADSL, the users are able to talk over telephone while enjoying broadband Internet access or data transmission at high speed (64k - 1Mbps for uploading and 256k - 12Mbps for downloading).

(2) Economic concern: The installation for the first time requires an installation fee, and the Internet access fee plus monthly rent is approximately NT$ 1,000 for the service at the transmission rate of 12M/1M (downloading/uploading). It is expected to be less expensive.

(3) Advantage: The advantage of using ADSL is that one can choose the transmission rate based on what one needs. For the high reliability and stability, 24-7 online access is not a problem. Most of the transmission is done through fiber optics network, resulting in a dramatic increase in both transmission rate and stability.

8. Monitoring data storage and management

It is expected that the BHMS will collect a huge amount of data. Manual reading of these data is time-consuming. Despite the introduction of automated monitoring in the Bridge, an information system that combines all data to provide a solid foundation for bridge behavior analysis and health and safety maintenance is yet to be developed. The primary purpose of the Bridge's monitoring system is to establish an in-situ data storage platform using Internet. Data can be measured on site in a reliable and effective way and an integrated information platform for data transmission, management and capturing is established to improve the performance of searching and capturing. For implementation, the entire system is Internet-based, free from the limits of platform or geometry. The time-history data measured can be recorded, converted, searched, displayed and downloaded, and the convenience of manipulating data for users is increased. Moreover, the data transmitted to the "bridge management database for Kao Ping Hsi Cable-Stayed Bridge" via regular remote data transmission link in 3 ways:

(1) Transmission of data via FTP at fixed intervals: the in-situ data storage system will transmit the compressed data through Internet link back to the data management system server at the appointed time.

(2) Remote data transmission: the system administer can retrieve the data using remote control program in case that the in-situ data storage fails to transmit the data at the appointed time.

(3) Manual data access: specific instruments will save the data in the data storage system onsite via data logger. These data can be downloaded manually at preset intervals and imported into the management system.

In addition, the data maintenance and analysis are very important to a long-term monitoring plan.

With the advancing of computer and Internet technology, the concept of remote control and centralized data management is taking shape. However, the biggest challenge is how to download, save, process and broadcast the monitoring data. As a result, the data storage is designed as follows for the monitoring data management:

(1) Monitoring data processing: includes data organization, format conversion and data analysis (such as Mean, RMS and so on).

(2) Monitoring data management: includes data storage and management, and the data management for special events (e.g. typhoons).

(3) Data display and access: includes time-history plotting and raw data downloading.

Also, the user interface must be easy to read, understand and use, and therefore an interface in Chinese is used.

3.4 Monitoring data transmission method and structure

The Bridge is a large-span bridge, which means that the monitoring spots are often far away from the monitoring office, resulting in greater signal attenuation and interference noise. Therefore, it is essential to select the right means to transmit signals. In the traditional way of analogue signal transmission, the signal attenuation and interference grow with the distance of transmission. To overcome such downsides, the distance of analogue signal transmission has to be limited to a certain range, and the analogue signals have to be amplified with signal conditioner before being transmitted, and then converted to digital signals for remote transmission.

With the advanced transmission technology, the more feasible signal transmission method is selected for this study, as shown in **Fig. 3.1**. This transmission works by converting the analogue signals sent out by the sensors through distributed digital module. The digital signals are not affected by signal attenuation or noise interference over a long distance (within 1km), and are capable of being transmitted over cables, resulting in a lower wiring cost. Furthermore, the distributed data transmission works by distributing or connecting several distributed digital modules and then transmitting to data capturing system to simplify the wiring and maintenance

procedure. At the end, the data is transmitted to the computer at the monitoring office via fiber optics network. The monitoring structure is shown in **Fig. 3.2**.

3.5 Principles for monitoring system scheduling

The monitoring system in this study is designed based on the following principles:

1. Due to limited budgets and lack of monitoring data, the entire monitoring is designed in one stage but installed in two. The stage one plan is the "system establishment and data collection," and the stage two plan is the "functional performance and practical implementation."
2. The stage one "system establishment and data collection" aims to establish the system structure and collect first data. The works include the installation of basic monitoring instrumentation required in the contract, system establishment, data recording, monitoring and preliminary data collection.
3. In stage two "functional performance and practical implementation," the aim is to combine both traffic control and the monitoring system to initiate the announcement of alarm for danger and bridge closing for the actions and purpose of bridge safety monitoring. The alarm values are established with the concept of multiple monitoring as the basis for traffic control and to increase the reliability of alarm announcement. Monitoring spots and items are increased based on safety control and practical functioning need for the goal of monitoring, control and safety.
4. While the monitoring system structure is developed, it is necessary to leave some room for expansion of instruments and wiring. It helps prevent maintenance costs and the compatibility concern in the integration of traffic control and the monitoring system, and avoids the complexity in the system operations and data collection in the future.

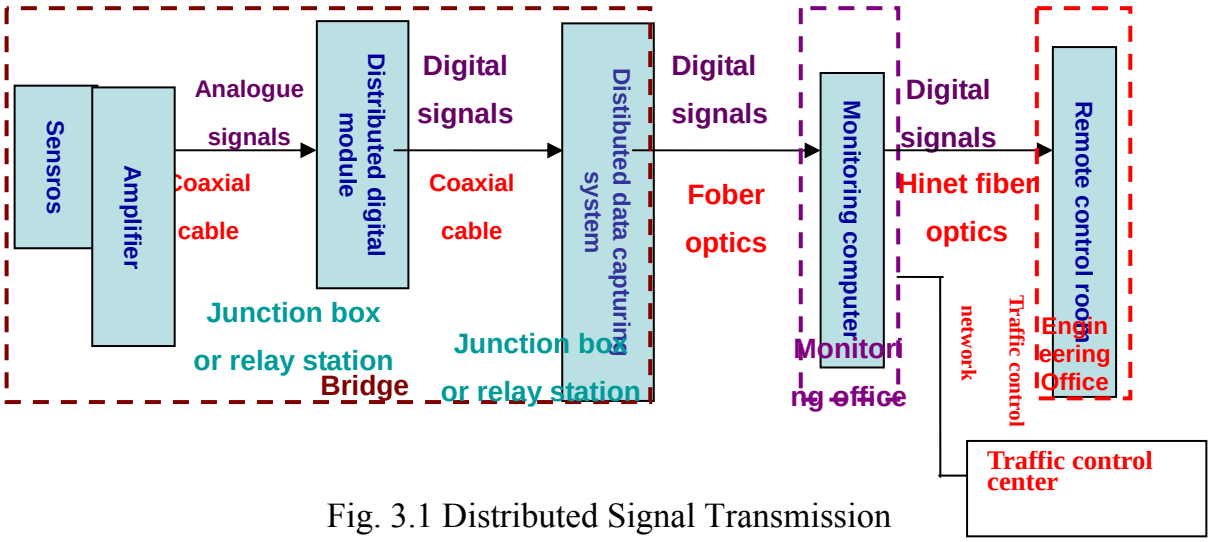

Fig. 3.1 Distributed Signal Transmission

3.6 Monitoring system design

For future expandability and convenience of maintenance and management, the distributed signal transmission is introduced in the system design. The monitoring of the entire system is designed to cover earthquakes, winds and traffic as the 3 major axes. An alarm capability focusing on "multiple safety monitoring" is established centering on dynamic monitoring aided with static monitoring. Also for future expandability, serviceability and cost down, the features of distributed transmission are put to good use. The overall dynamic and static monitoring system structure is shown in **Fig. 3.2**. **Table 3.1** gives the instruments used. The layout of instruments is shown in Fig. 1~7 in Attachment 1. The monitoring purpose and need corresponding to the monitoring instruments are shown in Attachment 2.

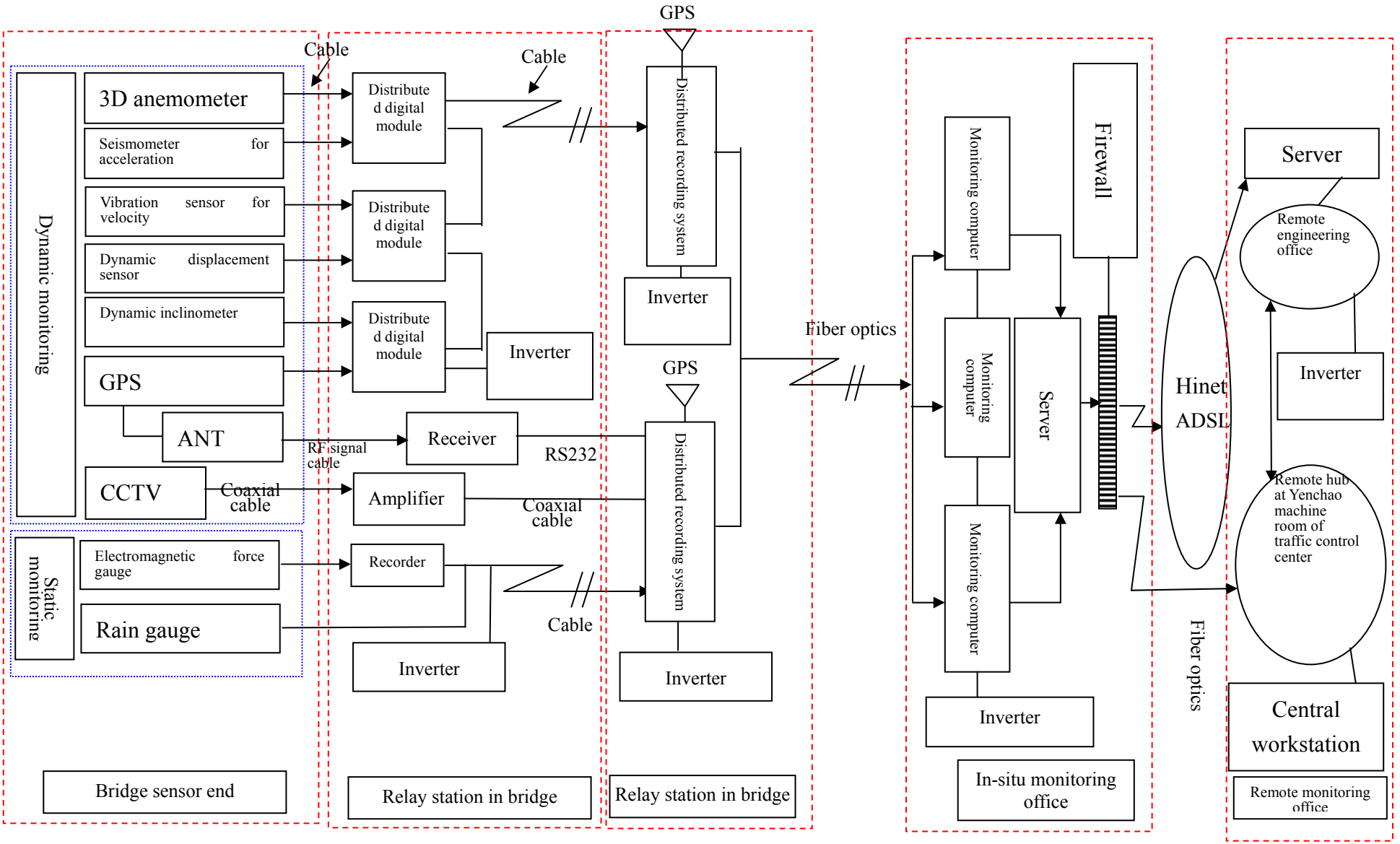

Figure 3.2 Monitoring System Structure

Table 3.1 Types and Number of Monitoring Instruments

Item	Name	Code	Mark	Unit	Qty	Remark
Dynamic sensors						
1	3D anemometer	ANM	★	Set	4	ANM01~ANM04
2	Embedded seismometer for acceleration (3-axis)	ACC	●	Set	1	ACC01
3	Surface-mounted seismometer for acceleration (3-axis)	ACC	●	Set	5	ACC02~ACC18
4	Surface-mounted seismometer for acceleration (uni-axial)	ACC	●	Set	12	
5	Vibration sensor for velocity (uni-axial)	VEL	■	Set	22	VEL01~VEL22
6	Dynamic displacement sensor (uni-axial)	DSP	◆	Set	6	DSP01~DPS06
7	Dynamic displacement sensor (3-axis)	TLT	⊕	Set	1	TLT01
8	GPA	GPS	▲	Set	5	GPS01~GPS05
9	Video monitoring system	CTV	▽	Set	4	CTV01~CTV04
	Dynamic sensors in total			Set	60	
Static sensors						
10	Electromagnetic force gauge	EMT	⊙	Set	4	EMT01~EMT04
11	Rain gauge	RAN	○	Set	2	RAN01~RAN02
	Static sensors in total			Set	6	
12	Dynamic video and data acquisition system	DRS	□	Set	1	DRS
13	Static video and data acquisition system	SRS	※	Set	1	SRS

4. Analysis and application of monitoring data

4.1 Measurement and establishment of initial monitoring values

(1). A two-moth test run follows the installation of the monitoring system. In-situ tests are carried out with all system functions in normal condition. Measurement with portable device and the system is conducted for comparison.

(2). The in-situ vibration test includes the measurement of main girder, tower and stay cable structure. A verified system identification is used to determine at least the first 5 natural

vibration frequencies at the 4 directions of girders and the tower, damping ratio and vibration states.

(3). Vibration method is used on 60 stay cables. The first 5 natural vibration frequencies of the cables are determined using the verified system identification, and the cable tensioning of the cables are determined using two or more calculation methods.

(4). A more reliable 3D full-bridge finite element analysis model is built based on the result of in-situ tests.

(5). Historic test data are collected to compare with test results for the development of initial monitoring parameters. The development is carried out as required by the engineering office.

(6). The contractor shall submit the initial monitoring parameter schedule to the engineering office for review and approval before the construction begins.

(7). In 2 months after the monitoring system is complete, the in-situ test of bridge measurement will start. In 3 months after the monitoring system is complete, the initial behavioral analysis of the Bridge shall be done and initial parameters developed. 3 copies of initial parameter evaluation report for the structure system shall be submitted to the client or construction supervisor for review.

4.2 Cable tensioning measurement and establishment

In engineering practice, the tensioning of cables is mostly calculated using the natural frequencies of the cable. Therefore, the examination of cable tensioning must be performed in coordination with vibration measurement, and then the tensioning force is determined with the frequencies measured. All the stay cables of the Bridge will be put to vibration tests under normal traffic with the Bridge in operation.

In general, the cable tensioning is calculated based on the analysis models developed from various assumptions. Those commonly used are:

(1). String vibration theory: Both ends of a cable are considered fixed, and the cable itself is

simulated as a wound-up string under only uniformly distributed tension with no consideration of bending moment. The string vibration equation gives the relation between tension and frequency:

$$T = \frac{4wl^2}{n^2 g} f_n^{\,2} \tag{4.2.1}$$

Where T is the tension force of the cable, w is the weight of cable per unit length, l is the length of cable, f_n is the *nth* natural vibration frequency (*Hz*), and g is the gravitational acceleration ($9.81 m/sec^2$).

(2). Beam vibration theory: A steel cable is considered as a simply supported beam under axial force with no consideration of geometrically nonlinear effects. The control equation showing the relation between lateral vibration frequency and axial force is derived to determine the relation between tension force and frequency as follows:

$$T = \frac{4wl^2}{n^2 g} f_n^{\,2} - \frac{n^2 EI\pi^2}{l^2} \tag{4.2.2}$$

Where E is the elastic modulus and I is the moment of inertia. Therefore by comparing Eq. (4.2.1) and Eq. (4.2.2), it is clear that the second term on the right-hand side of Eq. (4.2.2) is the effect when considering the flexural rigidity of the cable.

(3). Frequency difference formula: Connected to the decks of long span, the cables may be subject to the interference from the vibration of bridge decks. It is quite easy to make mistake by taking the low vibration frequency of the bridge deck as the real local frequency of the cable. Thus, according to the basic assumption of the vibration of wound-up string, the cable tension force is with the characteristics of equally spaced adjacent vibration frequencies, i.e. the difference between adjacent vibration frequencies (Chen et al., 2005[a]), to establish the relation between tension force and frequency difference Δf as follows:

$$T = \frac{4wl^2}{g} \Delta f^{\,2} \tag{4.2.3}$$

In practice, the first vibration frequency is usually substituted into Eq. (4.2.1) or (4.2.2) to determine tension force, i.e. n=1 and f_n=f_1. At this moment, it is learned by comparing Eq. (4.2.1) and (4.2.3) that **the frequency difference of cable is equal to the first vibration frequency**.

However, a cable is not a perfectly wound-up string structure. There are still nonlinear characteristics in it, such as flexural effect and sagging. As a result, difference still exists in the real-world measurement.

(4). **Nonlinear formula**: Considering that the contour of a cable is a parabola, and that the nonlinear effects, such as sagging, mass distribution and 3D inclination (Zui et al., 1996), a nonlinear transcendental equation is developed to determine a **calculation formula that divides cables into 3 types** based on the range of sagging, length and tension force of cable. However in practice, it is difficult to measure cable geometry such as sagging and inclining angle and it is necessary to determine the cable tension force using numeric iteration.

In practice, the calculation methods mentioned above all have their up and downsides, but the numeric difference is still within an acceptable range. Therefore, all three of them are widely used for cable tension calculation. The simple string theory equations (Eq. (4.2.1)), frequency difference equation (Eq. (4.2.2)) and beam theory equation (Eq. (4.2.3)) will be selected for the calculation of cable tension. For effective string length l_e, the effective string length is taken as the cable length l for cable tension calculation, as the actual string length of the cable is shorter than the entire length of the cable due to the clamping effect generated from the rubber dampers installed at the ends of cable. Chang (2000) measured the effective length of cables during the construction, as shown in **Table 4.1**. As a result, the effective string length will be used as the cable length for the tension calculation.

For the measurement and analysis of cable vibration, there are 60 stay cables distributed within 510 m along the Bridge. These cables are measured in 15 batches due to the limitation of the channels of the instruments used and the signal attenuation. For example, 14 channels are used in the first measurement. The cables measured in this batch are the two at B101, one at the southbound side (B101R) and the other at northbound side (B101L), and the two at B101A (B101AR and B101AL) for the vibration responses in three directions. This adds up to 12 channels. Also, a measurement spot is located at the decks of each of B101 and B101A for the vertical vibration at the deck, and 2 channels are used for these spots, as shown in **Fig. 2.3**. Each

of the measurements lasts **10 minutes**, and the frequency sampled is **100Hz**. Samples are taken at a total of **60,000 spots**. The measurement is the same for the rest of the cables. In addition, as the traffic cannot be blocked and the plan is running on the limited budget, no crane is used for this test. As a result, the measurement spots on the cables are located **2.5m** above the bridge decks, as shown in **Fig. 4.1**. To protect the HDPE sleeves around the cables, semi-circular jackets are produced according to the outer diameter of the cables. 3 uni-axial sensors are mounted on the flat surface of the jackets to measure the vibration of cables in 3 directions. Smaller responses are measured at the relatively low elevation due to the large vibration of cables, but no influence occurs on the analysis results.

Table 4.1 Cable Material and Geometry

Cable no.	Cable length l (m)	* Effective string length l_e (m)	*Mass, M (kg/m)	No. of strands (per cable)	*Rigidity, EI (kN-m^2)	Inclining angle θ (deg.)	Sagging δ (m)
B101A	220.121	213.338	152.7	91	2906.11	32.774	1.857
B101	220.785	214.897	152.7	91	2906.11	32.778	1.901
B102	208.825	202.376	129.9	69	1670.81	33.695	1.319
B103	197.117	190.612	143.4	82	2359.7	34.743	1.039
B104	185.491	178.897	137.2	76	2027.01	35.924	0.863
B105	173.953	167.258	129.9	69	1670.81	36.401	0.804
B106	162.548	155.727	144.4	83	2417.6	38.805	0.585
B107	151.286	144.326	149.6	88	2717.65	40.579	0.474
B108	140.21	133.07	134.1	73	1870.14	42.647	0.497
B109	129.386	122.119	136.1	75	1974.02	45.079	0.365
B110	119.02	111.195	128.9	68	1610.48	47.97	0.33
B111	108.549	100.658	96.8	57	1132.17	51.443	0.25
B112	99.137	90.256	83.3	44	689.43	55.66	0.245
B113	90.298	80.394	125.8	65	1502	60.824	0.221
B114	82.752	69.266	94.7	55	1041.98	67.172	0.155
F101A	326.788	319.287	130.9	70	1719.59	22.85	4.159
F101	328.837	322.086	130.9	70	1719.59	22.855	4.3
F102	307.418	300.5	100.9	61	1305.84	23.601	2.594
F103	287.497	280.593	132	71	1769.07	24.446	2.373
F104	267.657	260.778	133	72	1819.26	25.417	1.93
F105	247.901	239.92	128.9	68	1622.73	26.545	1.79

Cable no.	Cable length l (m)	* Effective string length l_e (m)	*Mass, M (kg/m)	No. of strands (per cable)	*Rigidity, EI (kN-m^2)	Inclining angle θ (deg.)	Sagging δ (m)
F106	228.267	221.427	144.4	83	2417.6	27.869	1.291
F107	208.782	201.945	148.5	87	2656.24	29.445	1.046
F108	189.488	182.649	139.2	78	2135.1	31.349	1.061
F109	170.467	163.603	135.1	74	1921.73	33.687	0.751
F110	151.719	144.937	125.8	65	1483.77	36.618	0.624
F111	133.273	126.792	93.7	54	1026.62	40.367	0.489
F112	117.056	109.397	82.3	43	654.01	45.317	0.452
F113	100.979	92.63	100.9	61	1302.57	51.988	0.247
F114	87.161	76.021	100.9	61	1281.72	61.147	0.378

Note: * The parameters shown in this column are taken from Chang, Yi-Hsiang (2001); the two cables at the same location have the same properties.

To determine the vibration frequency of cables, the spectrum of cables is obtained by putting the vibration time-history measured through fast Fourier transform (FFT), as shown in **Fig. 4.2~4.4**, which are the spectra of shorter cable (F114R), cable with medium length (F107R) and the longest cable (F101R) at the southbound side (S-R side) of the main span, respectively. The X, Y and Z axes in the figures are defined in **Fig. 2.1**. DZ is defined as the vertical vibration response of bridge decks at the joint between the respective cables and the deck. The cables have a circular, symmetric cross section, and it is reasonable to assume that the vibration frequencies at X-direction and Y-direction should be similar. However, difference may exist due to the nonlinear effects of the cables. Also, the cable vibration at Z-direction is susceptible to the (constraint parameter vibration between cable and bridge deck (Takahashi 1991), and it is difficult to determine the vibration mode of cables at low frequency. Therefore, it is very easy to tell the natural vibration frequencies of the cables at higher vibration modes in the spectra. On the other hand, it is difficult to tell the first a few frequencies at lower vibration modes. These conditions are attributed to the interference due to the vibration of bridge decks, and that is one of the reasons why the response of bridge decks has to be measured at the same time, as the cables and decks are

connected, which means that the frequencies measured on the cables may not only be those of the local vibration modes in the cables, but also those of the bridge decks. Hence, by measuring the vibrations in the cables and bridge decks simultaneously, the local vibration modes of the cables at lower frequencies are screened out to prevent misjudgment on the cable frequencies.

Figure 4.1 Mounting of Sensors at Three Directions

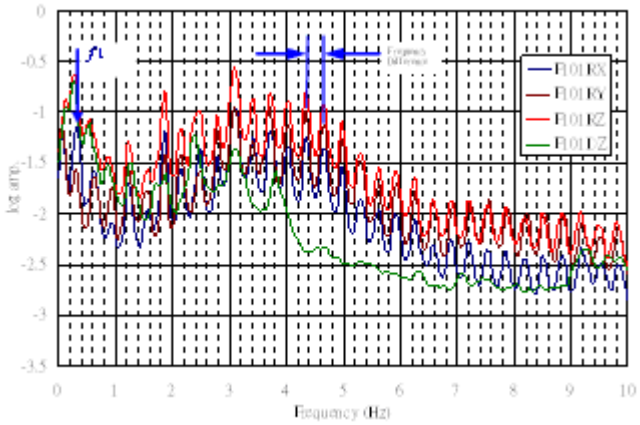

Figure 4.2 Spectrum of F101R cables (longest)

Suggested by Chen et al. (2005[b]), the **first 5 vibration frequencies at X-direction** are selected to calculate the tension in the 60 cables on southbound side (S-R side) and northbound side (N-L side), as shown in **Table 4.2**. The calculation includes:

1. To identify the first 5 vibration frequencies of the cables and calculate the tension according to the string theory. The average of the tension from these 5 frequencies is considered the tension of the respective cable. The analysis result is shown as T_1 in Table 2 and 3.
2. The use of the differences between the first 5 frequencies to calculate the tension. The average of tensions obtained from these 4 differences is considered as the tension of the respective cable.

The analysis result is shown as T_2 in Table 2 and 3.

3. The use of the first 5 frequencies to calculate cable tension using the beam theory. The average of these 5 tensions is considered as the tension of the respective cable. The analysis result is shown as T_3 in Table 2 and 3.

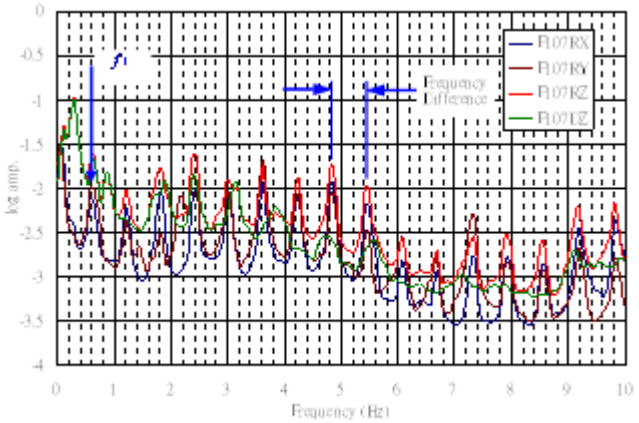

Figure 4.3 Spectrum of F107R Cables (cables with medium length)

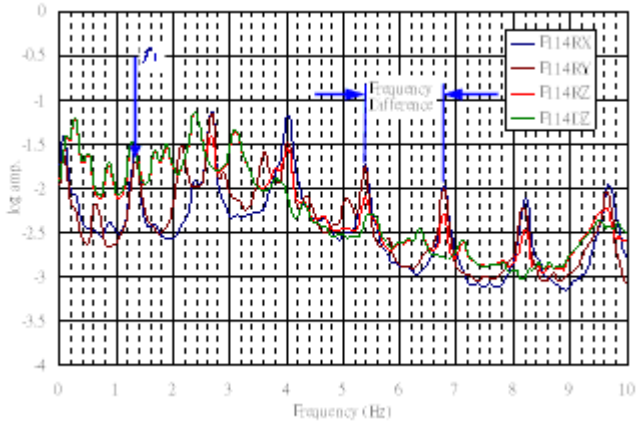

Figure 4.4 Spectrum of F114R Cables (short cables)

If based on the calculation of beam theory, the comparison between the results from different calculation methods suggests that the difference among the cable tensions calculated in these three methods is within a range of **0.5%**, indicating negligible difference between methods. However for the judgment of cable frequencies, the frequency difference method provides produces the correct frequencies more easily, and error in determining local frequencies of cable is relatively unlikely. Therefore in practice, the three methods for calculation of cable tension are acceptable, but it is more feasible and recommended to select more vibration frequencies to calculate the

tension and determine the average. Also it is found in the calculation that, for longer cables such as F101~F103 cables, when the first vibration frequency is used for tension calculation with the beam formula, the result displays a somewhat greater difference than those calculated with other vibration modes. Rather, tension calculation with higher vibration frequencies provides better convergence (Chen et al., 2005[b]). This is because of the apparent nonlinear effect of long cables. If the cable tension is calculated with the nonlinear equation, the longer cables will be placed in Type 2 or 3, which requires higher vibration modes for tension calculation. Greater error may exist if only the first vibration frequency is used for calculation of long cable tension. As a result, when calculating cable tension with the three methods mentioned above, it is prudent to calculate cable tension with more vibration frequencies and then the average tension, which should reduce the error in long cable tension calculation.

The curvature mode index and modal flexibility index, among others, are some of the indices commonly used for locating structure damage. However, these indices share a common problem that they require the vibration modes of the bridge and thus are more demanding in terms of in-situ measurement and system identification techniques. Also, it is not easy to control the measurement accuracy, particularly when high vibration mode parameters are required. The foregoing damage indexing is applicable to locating the damage of a cable-stayed bridge. However, being a highly statically indeterminate structure, a cable-stayed bridge features a complex cabling system that often leads to significant errors due to nonlinearity when an analysis model is built for such a bridge, and this nonlinearity in turn increases the difficulty in assessing the safety of a cable-stayed bridge. In reality, the behaviors of a cable-stayed bridge are read through how it is loaded. The main girders of bridge deck and cables are the primary elements that are susceptible to damage. The two are in fact connected, thus creating an inseparable correlation between them. Hence, if cable tension is obtained from cable measurement and testing, and the changes in the loading of cable are understood, it is possible to further evaluate the safety of bridge.

Figure 4.5 shows the distribution of tension in the 60 cables obtained using the beam theory. A tension index is developed from this:

$$TI(\%) = \frac{|T_L - T_R|}{T_L} \times 100\% \qquad (4.2.4)$$

Where T_L and T_R are the tension in the cables on the left side and right side, respectively, at the same location. Theoretically, the cables on both left and right sides of the same location should have tensions very close to one another. However, there may be some problem with the pair of cables if the difference of tension between the two is beyond a tolerable range. **5%** of allowable tolerance is assumed for this study. The cable tension at the *L* side is used as benchmark, and a defect may exist in the cables if that benchmark is exceeded.

As shown in **Figure 4.6**, the cables for which the allowable tolerance is exceeded are **B109R** and **B109L** cables with a difference of **33.40%**; **B111R** and **B111L** cables with a difference of **7.65%**; **B113R** and **B113L** cables with a difference of **6.99%**, and **F101R** and **F101L** cables with a difference of **6.09%**. Also, **Figure 4.6** suggests that if a defect is detected in the cable tension, the difference in *TI* will grow dramatically. Thus, the tension index is highly sensitive to damage and should be applicable as a damage index. As a result, in a case such as the Bridge, this index may be used as the judgment parameter of damage defects for a cable-stayed bridge having its cables arranged in this fashion, and an allowable tolerance percentage can be reasonably developed. In case that this tolerance is exceeded for the tension in the cables at both left and right sides of the same location, these cables should examined and evaluated, and so should the main girders of the bridge deck where the defect is found in the cable tension.

Figure 4.7 is the distribution of the first vibration frequency for the cables. A bell-shaped distribution is clear for the vibration frequencies, and this is consistent with the finding of Ren *et al.* (2005). Therefore, it is safe to say that a bell-shaped distribution is not the case for the frequencies of cables with defect, and this argument may be used for preliminary determination of where the damage is. However, **Figure 4.7** suggests this frequency distribution may not be sensitive enough to be used as a damage index.

Table 4.2 Results from the Tests of Cables at Southbound Side (S-R side)

Cable no.	f_1 (Hz)	f_2 (Hz)	f_3 (Hz)	f_4 (Hz)	f_5 (Hz)	Average frequency difference Δf (Hz)	Average cable tension (kN)		
							T_1	T_2	T_3
B101AR	0.51270	0.98877	1.48926	1.97754	2.47803	0.48828	6915.12	6828.18	6908.18
B101R	0.50049	0.97656	1.46484	1.94092	2.44141	0.49560	6776.45	6725.08	6769.62
B102R	0.52490	1.02539	1.53809	2.06299	2.57568	0.51514	5671.73	5647.22	5667.30
B103R	0.57373	1.13525	1.70898	2.27051	2.85645	0.57129	6770.89	6801.78	6763.84
B104R	0.63477	1.25732	1.89209	2.51465	3.17383	0.63476	7004.71	7076.93	6997.84
B105R	0.68359	1.33057	2.00195	2.67334	3.35693	0.66650	6548.85	6457.26	6542.37
B106R	0.78125	1.55029	2.33154	3.11279	3.89404	0.78125	8480.99	8549.39	8470.17
B107R	0.89111	1.77002	2.67334	3.56445	4.46777	0.89111	9881.80	9898.00	9867.63
B108R	0.84229	1.69678	2.55127	3.40576	4.26025	0.85449	6845.24	6935.30	6833.78
B109R	0.97656	1.96533	2.94189	3.91846	4.90723	0.98389	7800.12	7859.16	7785.74
B110R	1.03760	2.08740	3.13721	4.17480	5.26123	1.06201	6956.48	7190.22	6942.34
B111R	1.19629	2.39258	3.58887	4.79736	6.00586	1.19385	5629.34	5591.52	5617.21
B112R	1.33057	2.66113	4.00390	5.33447	6.68945	1.33789	4826.32	4858.45	4817.13
B113R	1.41602	2.85645	4.30908	5.76172	7.20215	1.44775	6672.21	6816.75	6646.98
B114R	1.84326	3.67432	5.50537	7.37305	9.24072	1.85303	6162.32	6240.42	6138.75
F101AR	0.34180	0.62256	0.92773	1.24512	1.55029	0.30518	5363.26	4971.22	5361.43
F101R	0.30518	0.62256	0.92773	1.23291	1.53809	0.31006	5163.40	5221.91	5161.60
F102R	0.39063	0.75684	1.14746	1.51367	1.89209	0.37598	5309.99	5151.82	5308.42
F103R	0.41504	0.79346	1.19629	1.58691	1.98975	0.39062	6688.08	6343.16	6685.64
F104R	0.43945	0.85449	1.28174	1.70898	2.13623	0.42481	6680.56	6528.82	6677.66
F105R	0.46387	0.91553	1.36719	1.83105	2.28271	0.45654	6234.86	6185.96	6231.80
F106R	0.51270	1.01318	1.52588	2.02637	2.53906	0.50781	7321.80	7302.88	7316.44
F107R	0.61035	1.20850	1.81885	2.42920	3.01514	0.60303	8903.33	8809.02	8896.26
F108R	0.61035	1.20850	1.81885	2.41699	3.03955	0.60791	6835.29	6864.56	6828.34
F109R	0.67139	1.33057	1.98975	2.66113	3.33252	0.66650	6422.44	6425.45	6414.64
F110R	0.69580	1.36719	2.05078	2.75879	3.45459	0.69092	5014.24	5046.06	5006.57
F111R	0.91553	1.80664	2.72217	3.62549	4.54102	0.90820	4969.58	4969.91	4962.65
F112R	1.00098	2.00195	3.00293	4.01611	5.04150	1.01074	3963.88	4024.86	3957.95
F113R	1.28174	2.56348	3.83301	5.12695	6.43311	1.28906	5690.71	5754.43	5674.23
F114R	1.34277	2.67334	4.02832	5.38330	6.77490	1.37451	4217.12	4406.72	4193.04

Note: The R that comes behind the cable number indicates the cable on the southbound side.

Table 4.3 Properties and Test Result of Cables at Northbound Side (N-L side)

Cable no.	f_1 (Hz)	f_2 (Hz)	f_3 (Hz)	f_4 (Hz)	f_5 (Hz)	Average of first 5 frequency differences Δf (Hz)	Average tension (kN)		
							T_1	T_2	T_3
B101AL	0.50049	0.98877	1.50146	1.97754	2.47803	0.49561	6868.87	6828.24	6861.94
B101L	0.50049	0.97656	1.46484	1.95313	2.44141	0.48584	6793.22	6658.04	6786.38
B102L	0.53711	1.04980	1.57471	2.09961	2.63672	0.52246	5929.44	5808.89	5925.01
B103L	0.58594	1.15967	1.73340	2.30713	2.89307	0.57861	7006.01	6977.25	6998.96
B104L	0.63477	1.26953	1.90430	2.53906	3.18604	0.63476	7087.90	7076.93	7081.02
B105L	0.67139	1.35489	2.03857	2.72217	3.40576	0.68359	6682.33	6792.65	6675.84
B106L	0.78125	1.57471	2.35596	3.14941	3.93066	0.78857	8642.33	8710.44	8631.51
B107L	0.90332	1.78223	2.68555	3.58887	4.49219	0.90088	10030.61	10116.09	10016.44
B108L	0.84229	1.68457	2.53906	3.39355	4.24805	0.85205	6794.77	6895.71	6783.31
B109L	0.84229	1.69678	2.55127	3.40576	4.26025	0.85449	5850.92	5927.90	5836.55
B110L	1.06201	2.11182	3.18604	4.27246	5.35889	1.07178	7216.89	7323.07	7202.75
B111L	1.24512	2.49023	3.72314	4.99268	6.26211	1.25732	6094.43	6201.92	6082.30
B112L	1.34237	2.68555	4.01610	5.37109	6.72607	1.34530	4891.03	4912.39	4881.84
B113L	1.48926	2.95410	4.46777	5.90082	7.47070	1.49902	7172.02	7308.11	7146.79
B114L	1.84326	3.66211	5.50537	7.36084	9.25293	1.86523	6153.38	6322.91	6129.80
F101AL	0.34180	0.62256	0.92773	1.23291	1.53809	0.30273	5326.98	4891.98	5325.15
F101L	0.26855	0.61035	0.91553	1.23291	1.53809	0.31494	4867.07	5387.71	4865.27
F102L	0.39063	0.74463	1.12305	1.50146	1.86768	0.37109	5188.16	5018.84	5186.59
F103L	0.41504	0.79346	1.19629	1.58691	1.98975	0.39551	6688.08	6502.77	6685.64
F104L	0.43945	0.85449	1.26953	1.69678	2.12402	0.42236	6621.67	6453.98	6618.77
F105L	0.46387	0.82773	1.37939	1.81885	2.29492	0.46143	6026.58	6319.02	6023.52
F106L	0.52490	1.01318	1.52588	2.03857	2.55127	0.50781	7425.13	7302.88	7419.78
F107L	0.61035	1.19629	1.79443	2.40479	3.00293	0.60059	8770.30	8737.82	8763.23
F108L	0.61035	1.20850	1.81885	2.46990	3.01514	0.60303	6873.36	6754.74	6866.41
F109L	0.65918	1.30615	1.96533	2.63672	3.29590	0.65918	6246.36	6285.01	6238.56
F110L	0.68359	1.36719	2.05078	2.73438	3.43018	0.68848	4946.71	5010.48	4939.04
F111L	0.91553	1.80664	2.70996	3.61328	4.54102	0.90820	4954.04	4969.91	4947.11
F112L	1.02539	2.03857	3.06396	4.08936	5.13916	1.02783	4125.00	4162.12	4119.07
F113L	1.30615	2.61230	3.93066	5.24902	6.59180	1.32568	5948.64	6086.04	5932.16
F114L	1.34277	2.69775	4.06494	5.45654	6.86035	1.39649	4292.66	4548.74	4268.58

Note: The L that comes behind the cable number indicates the cable on the northbound side.

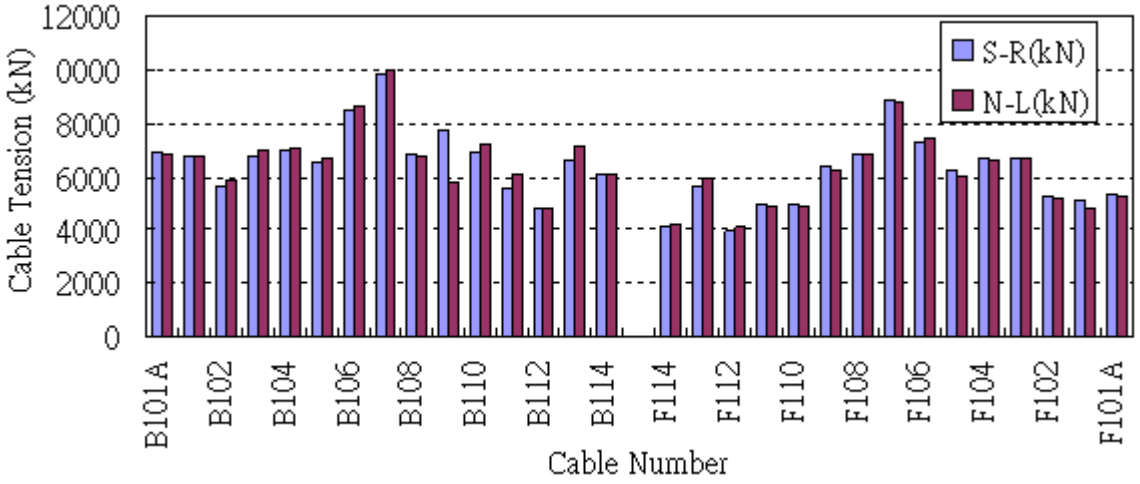

Figure 4.5 Distribution of Cable Tension: Southbound Side (S-R) vs. Northbound Side(N-L)

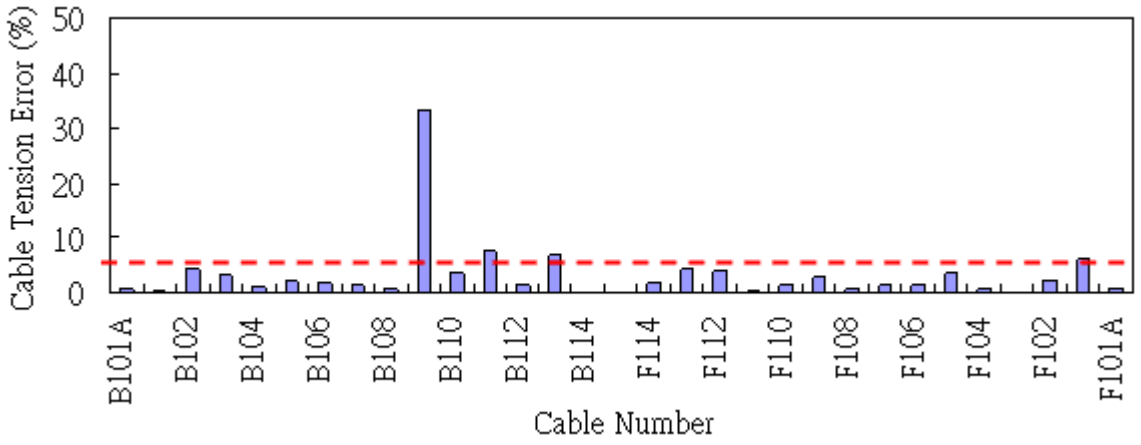

Figure 4.6 Cable Tension Tolerance: Southbound Side (S-R) vs. Northbound Side(N-L)

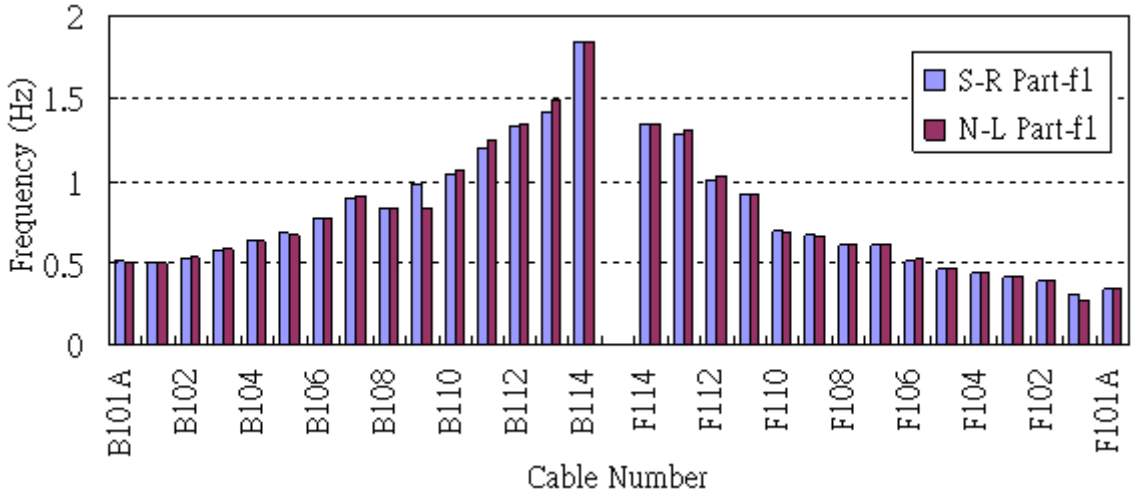

Figure 4.7 Distribution of First Frequencies of Cable: Southbound Side (S-R) vs. Northbound Side(N-L)

4.3 Measurement and establishment of the dynamic characteristics of the Bridge

The in-situ vibration tests are conducted on the Bridge. Continuous wavelet transform (CWT) is used for modal identification. As the wavelet transform has the advantage in both time and frequency domains, an effect similar to filtering in frequency domain is created by selecting dimensional parameters when transforming dynamic response into wavelet domain. By substituting in the time series model, similar to the procedure for traditional time series modeling, the parameters related to time series model are estimated, and the dynamic characteristic parameters, such as natural frequencies, damping ratio and mode shape, are determined. Also, the identification results are compared with the finite element model to obtain a finite element model that meets the real structure for the study of in-situ monitoring to come.

The identification using CWT is introduced to process the vibration test data of the Bridge for modal identification and determination of dynamic characteristic parameters of the Bridge. The method is selected for its advantages in both time and frequency domain. Filtering is conducted by selecting dimensional parameters when transforming dynamic response into wavelet domain (similar to filtering in frequency domain). By substituting in the time series model, the parameters related to time series model are estimated (similar to the procedure for traditional time series modeling). This method is used for processing the response from the vibration measurement to confirm its applicability. The data processing procedure starts by transforming the random vibration response to free attenuation response using random decrement method, followed by the establishment of AR model based on the result; and finally, the coefficients of AR model are used to estimate the modal parameters of the structure system. The frequencies, damping ratio and mode shapes are determined.

For the in-situ vibration tests, the main span of the Bridge is 330m long, and the side span is 180m. It is the longest cable-stayed bridge in the country. The vibration tests are conducted to measure the dynamic response of the main girders under normal traffic. The Bridge is not closed during the tests. Thus, the random traffic effect exists. In general, the normal traffic effect has no influence on the result of vibration tests conducted on the Bridge. Furthermore, for the setup of measurement stations, the primary considerations are the layout of nodes for finite element

analysis, the locations of cables and the installation of bridge sections. 33 measurement stations are established along the 510m length of the Bridge. Also due to the limits of number of channels available for the data acquisition system and the quantity of sensors, the 33 stations have to be measured in 3 segments, as shown in **Fig. 4.8**. Segment 1 is the measurement of main span, and the stations are located at Pier P2, 20m from P2, and the anchorage of cables from F101 to F110 on the bridge decks, 12 stations in total. Segment 2 is the measurement of partial main span and partial side span, and the stations are located at Tower P1, 20m in front of and 14.8m behind P1, the anchorage of cables from F109 to F114 and B114 to B112 on the bridge decks, 12 stations in total. Segment 3 is the measurement of side span, and the stations are located at Pier A1 and the anchorage of cables from B102 to B113 on the bridge decks, 13 stations in total. The arrangement above shows that Segments 1 and 2 overlap at the stations at F109 and F110, and Segments 2 and 3 at B112 and B113. There are 33 stations in total. The overlapping stations are established for the linkage of data for each segment. The vibration tests are conducted in the vertical direction (Z) and lateral direction (Y) to measure the response signals of vibration velocity at each of the two directions. The duration of measurement is 10 minutes, and the sampling frequency is 100Hz. 60,000 pieces of data are collected.

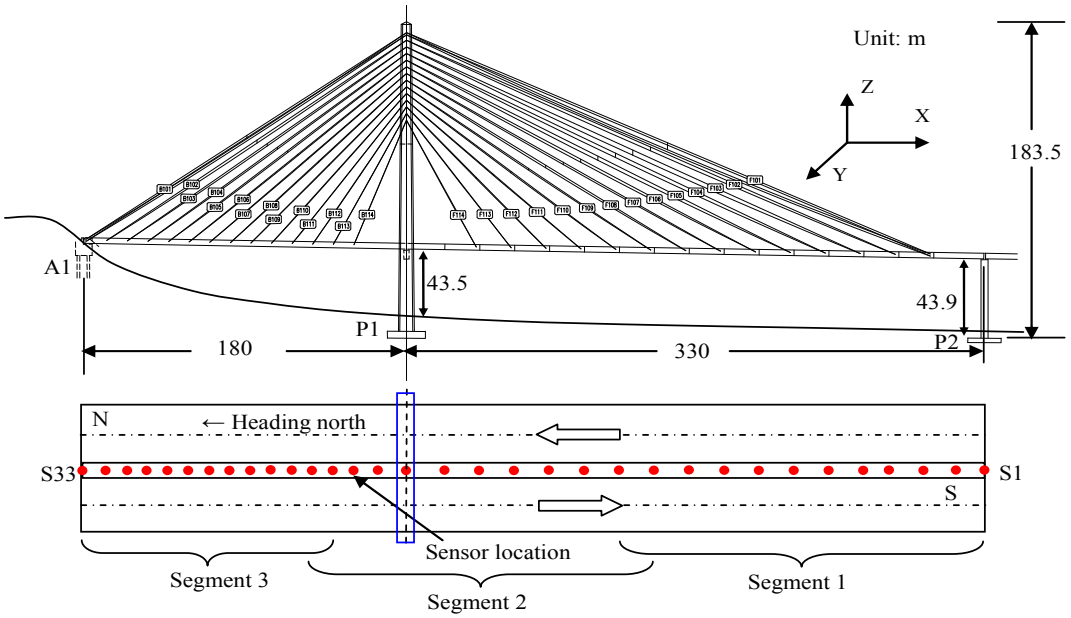

Figure 4.8 Layout of Measurement Stations along the Bridge

For system identification, CWT is used for the identification of dynamic characteristics. $L^2(R)$ is a square-integrable function space. A function $f(t)$ located in a space $L^2(R)$ is wavelet-transformable, and defined as:

$$W_f(a,b)=\left\langle f,\psi_{(a,b)}\right\rangle=|a|^{\frac{-1}{2}}\int_R f(t)\psi^*\left(\frac{t-b}{a}\right)dt \tag{4.3.1}$$

The inverse transform is:

$$f(t)=\frac{1}{C_\psi}\int_{-\infty}^{\infty}\int_{-\infty}^{\infty}\frac{1}{a^2}W_f(a,b)\psi\left(\frac{t-b}{a}\right)dadb \tag{4.3.2}$$

Where

$$C_\psi=\int_R\frac{|\hat{\psi}(\omega)|^2}{\omega}d\omega \tag{4.3.3}$$

$\psi(t)$ is the mother wavelet; $\psi_{(a,b)}(t)=\frac{1}{\sqrt{a}}\psi\left(\frac{t-b}{a}\right)$ is the basis function determined by expanding, contracting and shifting the mother wavelet function $\psi(t)$; a and b are the scale factor and shift factor, respectively; $\hat{\psi}(\omega)$ and $\psi^*(t)$ are the Fourier transform and conjugate function, respectively. The basis function mentioned above is contrary to that of the Fourier transform, which is fixed at $e^{i\omega t}$, and multiple selections are available for the mother wavelet function of the wavelet transform. However, the mother wavelet selected must fulfill:

(1). That the $\psi(t)$ and its derivatives of each order belongs to $L^\infty(R)$; and

(2). That the $\psi(t)$ and its derivatives of each order decrease dramatically when $t\to\infty$; i.e. the support length is limited.

According to the definition of Eq. (1), if $\psi(t)$ is considered as a window function with the center at t^* and a radius of Δ, and then the center of $\psi_{(a,b)}$ is at $b+at^*$ and the radius is $a\Delta$. Therefore, the wavelet transform expressed as Eq. (1) provides a signal $f(t)$ that contains partial information of a tie window:

$$\left[b+at^*-a\Delta,b+at^*+a\Delta\right] \tag{4.3.4}$$

This window is narrower for a small value of a, but wider for a large value of a. The window center and radius in Eq. are defined as:

$$t^* = \frac{1}{\|f\|^2}\int_{-\infty}^{\infty} t|f(t)|^2 dt \tag{4.3.5}$$

$$\Delta = \frac{1}{\|f\|}\left\{\int_{-\infty}^{\infty}(t-t^*)|f(t)|^2 dt\right\}^{\frac{1}{2}} \tag{4.3.6}$$

Where $\|f\|^2 = \int_{-\infty}^{\infty}|f(t)|^2 dt$. As

$$\frac{1}{2\pi}\hat{\psi}_{(a,b)}(\omega) = \frac{a|a|^{\frac{-1}{2}}}{2\pi}e^{ib\omega}\hat{\psi}(a\omega) \tag{4.3.7}$$

If $\hat{f}$ is the function of $f(t)$ that is transformed to the frequency domain using Fourier transform, the Parseval identity can prove that $\sqrt{W_f}(a,b)$ can be used to determine that $\hat{f}$ contains the partial information of a frequency window:

$$\left[\frac{\omega^*}{a} - \frac{\hat{\Delta}}{a}, \frac{\omega^*}{a} + \frac{\hat{\Delta}}{a}\right] \tag{4.3.8}$$

Where ω^* and $\hat{\Delta}$ are the center and radius, respectively, of $\hat{\psi}$ calculated using Eq. (4.3.5) and (4.3.6). This window has a center frequency of $\frac{\omega^*}{a}$ and band width of $\frac{2\hat{\Delta}}{a}$. Thus, the use of Eq. (4.3.1) for wavelet transform yields a time-frequency window:

$$\left[b + at^* - a\Delta, b + at^* + a\Delta\right] \times \left[\frac{\omega^*}{a} - \frac{\hat{\Delta}}{a}, \frac{\omega^*}{a} + \frac{\hat{\Delta}}{a}\right] \tag{4.3.9}$$

From all of the above, it is learned that the rectangular shape of the time-frequency window defined in $\psi_{a,b}(t)$ changes with the contraction-expansion factor, a. When a is small, it is a high frequency window with a narrow time width but large bandwidth that is perfect for describing high-frequency signals; when a is large, it is a low frequency window with a large time width but a narrow bandwidth good for describing low-frequency signals. As the wavelet function $\psi(t)$ is a band-pass function, the analysis above suggests that the change in the contraction-expansion factor a, $\psi_{a,b}(t)$, which corresponds to a series of bandwidth and center frequencies, is also a band-pass system.

Also during the CWT, there are many wavelet functions to choose from, such as Haar wavelet, Morlet wavelet, Meyer wavelet, and so on. The Meyer wavelet function is selected as the CWT basis function for this study. The mother wavelet function for Meyer wavelet is defined in the

frequency domain as:

$$\hat{\psi}(\omega)=\begin{cases}(2\pi)^{-\frac{1}{2}}e^{\frac{jw}{2}}\sin\left(\frac{\pi}{2}\nu\left(\frac{3}{2\pi}|\omega|-1\right)\right) & \frac{2\pi}{3}\le\omega\le\frac{4\pi}{3}\\ (2\pi)^{-\frac{1}{2}}e^{\frac{jw}{2}}\cos\left(\frac{\pi}{2}\nu\left(\frac{3}{2\pi}|\omega|-1\right)\right) & \frac{4\pi}{3}\le\omega\le\frac{8\pi}{3}\\ 0 & |\omega|\notin\left[\frac{2\pi}{3},\frac{8\pi}{3}\right]\end{cases} \tag{4.3.10}$$

Where $\nu(s)$ is the auxiliary function for the establishment of Meyer wavelet, which is expressed as:

$$\nu(s)=s^4\left(35-84s+70s^2-20s^3\right)\quad s\in[0,1] \tag{4.3.11}$$

The Meyer wavelet is not with compact support in time domain, but it is fast to converge to zero; i.e.

$$|\psi(t)|\le C_n\left(1+|t|^2\right)^{-n} \tag{4.3.12}$$

Where $\psi(t)$ is an infinite integratable function. The wavelet function of Meyer wavelet is shown in **Fig. 4.9**. During the identification, the scale factors of wavelet function can be set for the frequencies to be determined. The frequency reserve range suggested for Meyer wavelet function is $\left[\frac{0.5348}{a},\frac{0.9311}{a}\right]$.

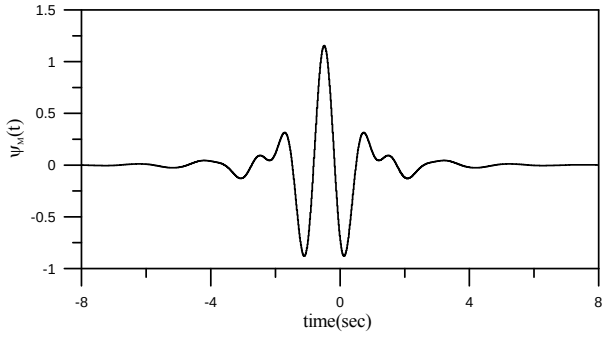

(a)

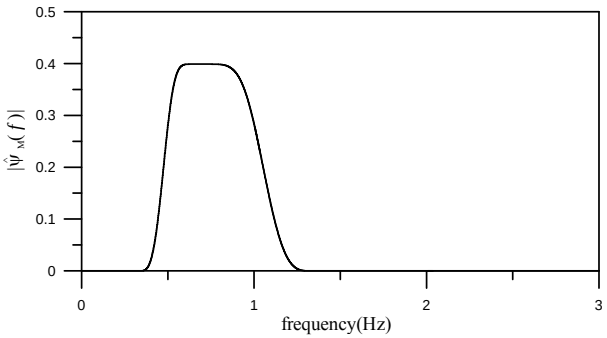

(b)

Figure 4.9 Meyer wavelet function: (a) time domain; (b) frequency domain

As there are too many source of eternal loading input for the vibration test, these external loads, if combined, are considered as a white noise. Thus, the vibration signals are converted to free attenuation vibration signals using random decrement technique, and the time series ARX model can be developed by assuming the external loads equal to 0. As a result, they can be converted to free attenuation vibration signals using random decrement technique for analysis. In a linear system, the response between degrees of freedom (or stations) measured can be expressed as:

$$\{y(t)\} = \sum_{i=1,2}^{I} [\Phi]_i \{y(t-i)\} + \sum_{j=0,1}^{J} [\Theta]_j \{f(t-j)\} \tag{4.3.13}$$

Where $\{y(t-i)\}$ and $\{f(t-i)\}$ are the response (acceleration or velocity) obtained at the measurement of the degrees of freedom in the structure and the external load inputted, respectively, at $t - i\Delta t$; $[\Phi]_i$ and $[\Theta]_j$ are specific coefficient matrices. There is no external load input for the vibration signals processed. If the vibration measurement signals are converted to free attenuation vibration signals using random decrement, Eq. (4.3.13) is rewritten as:

$$\{\bar{y}(t)\} = \sum_{i=1,2}^{I} [\Phi]_i \{\bar{y}(t-i)\} \tag{4.3.14}$$

Where $\{\bar{y}(t)\}$ is the free attenuation vibration signal of $\{y(t)\}$ using random decrement. With the wavelet transform using Eq. (4.3.1) and the translation invariance between the wavelet transform of $f(t-\tau)$ and $f(t)$, Eq. (4.3.14) is expressed as:

$$W_{\{\bar{y}\}}(a,b) = \sum_{i=1}^{I} [\Phi]_i W_{\{\bar{y}\}}(a,b-i) \tag{4.3.15}$$

To analyze the response measured within a specific frequency range, specific a and different b can be selected to determine the following with Eq. (4.3.15):

$$\{Y^{(0)}\} = [\tilde{C}]\{Y\} \tag{4.3.16}$$

Where the coefficient matrix $[\tilde{C}]$ is an unknown matrix determined using the least square error.

To estimate the dynamic characteristics of the structure system (e.g. natural vibration

frequencies, modal damping ratio and vibration shape), Eq. (4.3.13) can determine the coefficient matrix $[\Phi]_i \quad (i=1,2\cdots I)$. Therefore, if the k^{th} characteristic value of the system matrix is expressed as a_k+ib_k, then the kth undamped natural frequency and modal damping ratio are correlated to a_k and b_k, and the mode shape of the system is determined using the characteristic vectors.

For the test result and system identification result, shown in **Fig. 4.10** and **Fig. 4.11** are the vertical and lateral spectra, respectively, of the measurement station located at the anchorage of F104~F106 cables on the bridge deck obtained from the vibration test. For data processing, the vibration signals of the Bridge have to be converted to free attenuation vibration signals using random decrement, and the Bridge's dynamic characteristics are identified by using Meyer wavelet function as the basis function of the CWT. The scale factors used in the identification are shown in **Table 4.4**. The first 5 modal frequencies and damping ratios identified in each of the directions are shown in **Table 4.** and **Table 4.6**. The first lateral frequency from the vibration test shown in **Table 4.5** is 0.643Hz and the damping ratio is 3.3%; while the first lateral frequency obtained from the finite element analysis is 0.646Hz. The identification of natural frequencies and the analysis of FE model both yield similar results, and the damping ratio does not increase with frequency. It is learned from the vertical identification result shown in **Table 4.6** that the first vertical frequency from the vibration test is 0.284Hz and the damping ratio is 2.9%; whereas the first vertical frequency from finite element analysis is 0.293Hz. The results from both the identification and FE analysis are very close for other frequencies. In addition, it is observed in the vertical and lateral modal frequencies that the coupling vibration of the Bridge is not significant in either direction.

For the comparison of mode shape, the mode shapes identified in both directions are compared to those obtained from FE analysis, as shown in **Fig. 4.13 and Fig. 4.14**. The figures show that the first 5 mode shapes in either direction are similar between the result of identification and the analysis of finite element model. When the identification result is evaluated using MAC value, as shown in **Table 4.5 and Table 4.6**, the MAC value corresponding to each mode will be greater than 0.95, indicating that the result from analysis model is consistent with the actual bridge

characteristics.

Table 4.4 Scale Factors

Mode	1	2	3	4	5
Lateral	1.13	0.44	0.34	0.28	0.24
Vertical	2.50	1.31	0.79	0.49	0.48

Table 4.5 Lateral mode identification vs. finite element analysis result

mode	FEM	Ambient test		MAC
	Freq.(Hz)	Freq.(Hz)	damping ratio (%)	
1	0.293	0.284	2.9	0.99
2	0.561	0.574	3.7	0.99
3	0.931	0.922	4.4	0.95
4	1.52	1.54	3.9	0.98
5	1.79	1.81	3.0	0.97

Table 4.6 Vertical mode identification vs. finite element analysis result

mode	FEM	Ambient test		MAC
	Freq.(Hz)	Freq.(Hz)	Damping ratio (%)	
1	0.646	0.643	3.3	0.99
2	1.40	1.64	2.9	0.96
3	2.16	2.17	3.2	0.98
4	2.63	2.51	2.5	0.98
5	3.02	3.13	3.9	0.96

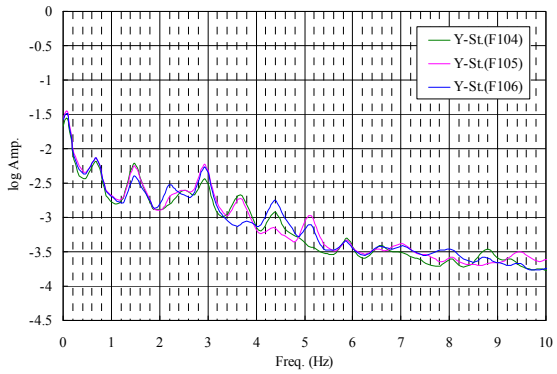

Figure 4.10 Lateral vibration test spectrum

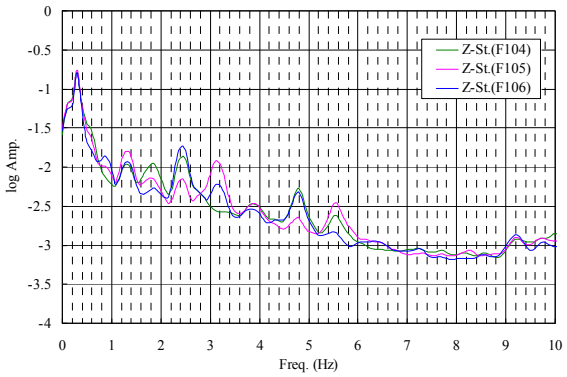

Figure 4.11 Vertical vibration test spectrum

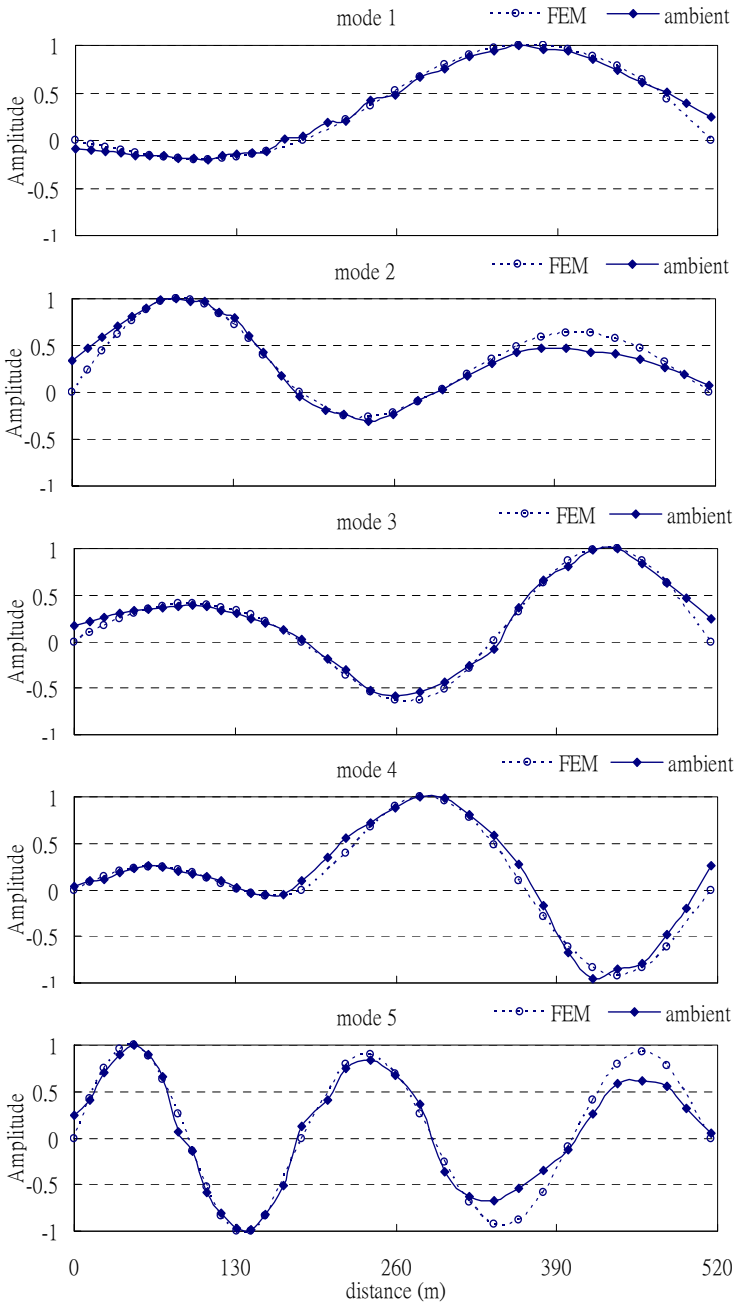

Figure 4.12 Mode shape: lateral vibration test vs. finite element analysis

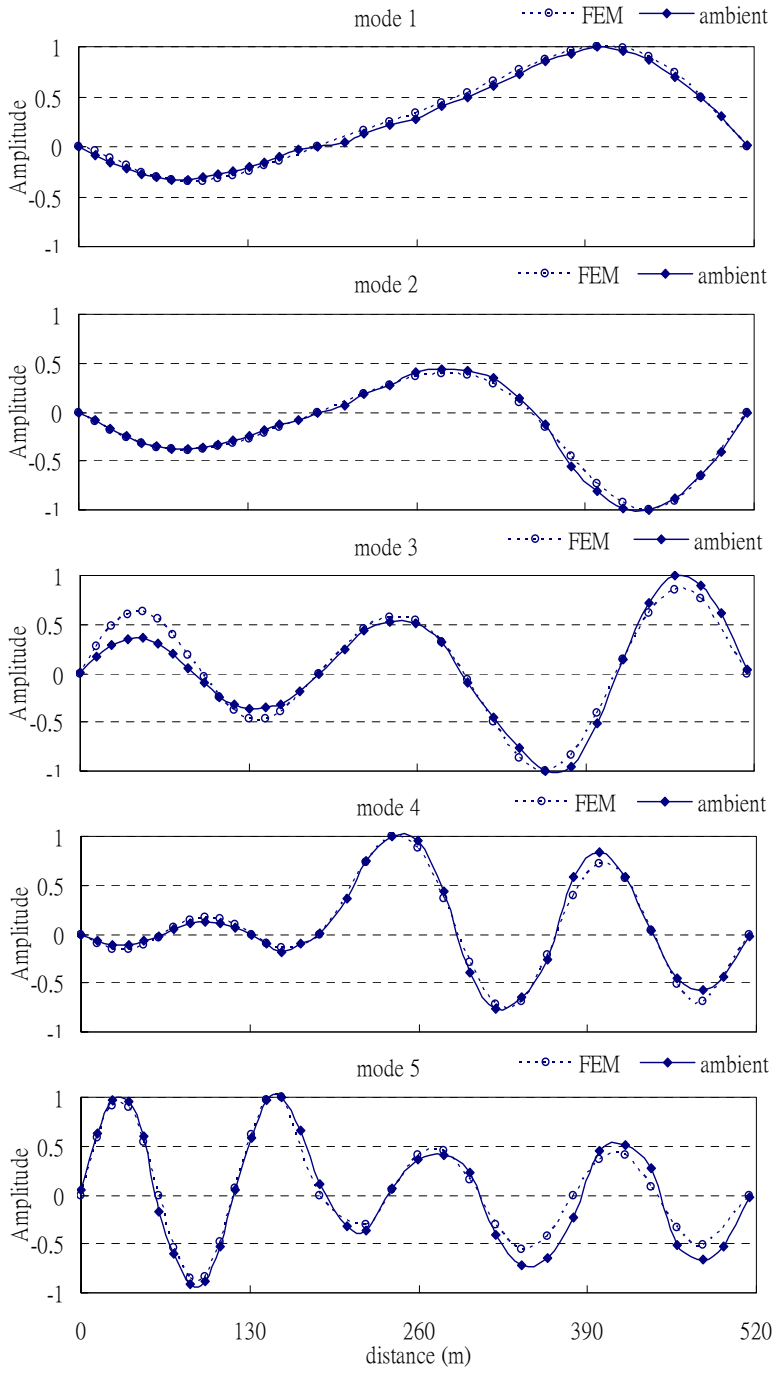

Figure 4.13 Mode shape: vertical vibration test vs. finite element analysis

As shown above, in-situ vibration tests are conducted on the Bridge. By using CWT for mode identification, it is feasible to identify the dynamic characteristic parameters of a cable-stayed bridge from the vibration test results. At the same time, it is identified that the dynamic characteristic parameters for the first 5 modes of the Bridge in lateral and vertical directions are consistent with those of the numeric analysis model established. The MAC values of mode shape

are all greater than 0.9, indicating that the analysis model built for the study should make sense and can be provided for in-situ monitoring and analysis in the future.

4.4 Analysis and establishment of aerodynamic characteristics of the Bridge

When a 3D bridge is subject to winds, its movement equation can be expresses in matrix as follows:

$$[\mathbf{M}]\{\ddot{D}(t)\}+[\mathbf{C}]\{\dot{D}(t)\}+[\mathbf{K}]\{D(t)\}=\{\overline{F}(t)\} \tag{4.4.1}$$

Where $\{D(t)\}$ is the displacement vector of the structure, $\{\dot{D}(t)\}$ and $\{\ddot{D}(t)\}$ are the velocity and acceleration vectors, respectively, $\{\overline{F}(t)\}$ is the load vector of the structure, and [**M**], [**C**] and [**K**] are the mass, damping and stiffness matrices of the structure, respectively. If the displacement vector is expressed in mode shapes, then by using the orthogonality of the mode shape function, the motion equation of the mth mode of the structure can be rewritten as:

$$M_m^*[\ddot{X}_m(t)+2\xi_m\omega_m\dot{X}_m(t)+\omega_m^2X_m(t)]=\{\overline{\phi}_m\}^T\{\overline{F}\ (t)\} \tag{4.4.2}$$

Where $\{\overline{\phi}_m\}$ is the shape function matrix of the mth mode; $\{X\}$ is the generalized coordinate vector; $M_m^*=\{\overline{\phi}_m\}^T[M]\{\overline{\phi}_m\}$; and ξ_m and ω_m are the damping ratio and angular frequency of the structure at the mth mode.

In general, the tower and cables are subject to smaller wind loads than the deck. Therefore, the impact of wind load on those two is negligible. Only the aerodynamics of the bridge deck is considered. According to the approach of Scanlan and Tomko (Scanlan and Tomko 1971), when the cross section of a bridge is subject to wind loads, the external forces sustained are analyzed in terms of self excited force and buffeting force. The components at vertical, leeward and torsional directions when the self excited force is acting on the bridge node *i* are expressed as:

$$L_{si}(t)=\frac{1}{2}\rho U^2(2B)(K)[H_1^*(K)\frac{\dot{y}(t)}{U}+H_2^*(K)\frac{B\dot{\alpha}(t)}{U}+KH_3^*(K)\alpha(t)]\Delta L_i \tag{4.4.3}$$

$$D_{si}(t)=\frac{1}{2}\rho U^2(2B)(K)[P_1^*(K)\frac{\dot{z}(t)}{U}+P_2^*(K)\frac{B\dot{\alpha}(t)}{U}+KP_3^*(K)\alpha(t)]\Delta L_i \tag{4.4.4}$$

$$M_{si}(t)=\frac{1}{2}\rho U^2\left(2B^2\right)(K)[A_1^*(K)\frac{\dot{y}(t)}{U}+A_2^*(K)\frac{B\dot{\alpha}(t)}{U}+KA_3^*(K)\alpha(t)]\Delta L_i \tag{4.4.5}$$

The footnote s denotes the self excited force, ΔL_i is the length of bridge deck at node *i* where the force concentrates, *y*, *z* and α are the displacements at vertical, leeward and torsional directions; $H_i^*(K)$, $P_i^*(K)$ and $A_i^*(K)$ (*i*=1, 3) are dimentionless aerodynamic parameters, $K=B\omega/U$ is the dimentionless frequency, $\omega=2\pi n$; *B* is the width of bridge deck; ρ is the density of air; and *U* is the average wind speed. Also, the buffeting force caused by turbulence is expressed as:

$$L_{bi}(t)=\frac{1}{2}\rho U^2 B\{C_L(\alpha_0)\frac{2u(x,t)}{U}+[\frac{\partial C_L}{\partial\alpha}\Big|_{\alpha=\alpha_0}+\frac{A}{B}C_D(\alpha_0)]\frac{w(x,t)}{U}\}\Delta L_i \tag{4.4.6}$$

$$D_{bi}(t)=\frac{1}{2}\rho U^2 B C_D(\alpha_0)\frac{A}{B}\left(\frac{2u(x,t)}{U}\right)\Delta L_i \tag{4.4.7}$$

$$M_{bi}(t)=\frac{1}{2}\rho U^2 B^2\{[C_M(\alpha_0)+C_D(\alpha_0)\frac{Ar}{B^2}]\frac{2u(x,t)}{U}+\frac{\partial C_M}{\partial\alpha}\Big|_{\alpha=\alpha_0}\frac{w(x,t)}{U}\}\Delta L_i \tag{4.4.8}$$

The footnote *b* denotes the turbulence effect, *u* and *w* are the disturbed wind speed at leeward and vertical directions, respectively, C_D, C_L and C_M are the static wind load coefficients at the leeward, vertical and torsional directions, respectively, α_0 is the average wind attack angle, $\frac{\partial C_D}{\partial\alpha}\Big|_{\alpha_0}$ and $\frac{\partial C_M}{\partial\alpha}\Big|_{\alpha_0}$ are the slope of curvature of C_D and C_M at α_0; *A* is the projection area of bridge deck per unit length on the vertical direction; and *r* is the distance from the center of mass of the bridge deck to the effective axis of gyration. The average wind attack angle is considered as 0 for this study, i.e. $\alpha_0 = 0$.

For wind load simulation, inverse Fourier transform is used to transform spectral functions into time histories. However, the number of time histories is limited to the size of frequencies sampled. Thus, the time histories obtained are not continuous. The time history series will be built using multiple-point autoregressive model for this study. The vectorized autoregressive model (AR(*p*)) can be expressed as:

$$\overline{\mathbf{Z}}_t=\Phi_1\overline{\mathbf{Z}}_{t-1}+\Phi_2\overline{\mathbf{Z}}_{t-2}+\cdots+\Phi_p\overline{\mathbf{Z}}_{t-p}+\mathbf{a}_t \tag{4.4.9}$$

By expressing Eq. (4.4.9) in 3-point pattern, it can be rewritten as:

$$\begin{bmatrix}\overline{Z}_{1,t}\\ \overline{Z}_{2,t}\\ \overline{Z}_{3,t}\end{bmatrix}=\begin{bmatrix}\phi_{11} & \phi_{12} & \phi_{13}\\ \phi_{21} & \phi_{22} & \phi_{23}\\ \phi_{31} & \phi_{32} & \phi_{33}\end{bmatrix}_1\begin{bmatrix}\overline{Z}_{1,t-1}\\ \overline{Z}_{2,t-1}\\ \overline{Z}_{3,t-1}\end{bmatrix}+\begin{bmatrix}\phi_{11} & \phi_{12} & \phi_{13}\\ \phi_{21} & \phi_{22} & \phi_{23}\\ \phi_{31} & \phi_{32} & \phi_{33}\end{bmatrix}_2\begin{bmatrix}\overline{Z}_{1,t-2}\\ \overline{Z}_{2,t-2}\\ \overline{Z}_{3,t-2}\end{bmatrix} \tag{4.4.10}$$
$$+\cdots+\begin{bmatrix}\phi_{11} & \phi_{12} & \phi_{13}\\ \phi_{21} & \phi_{22} & \phi_{23}\\ \phi_{31} & \phi_{32} & \phi_{33}\end{bmatrix}_p\begin{bmatrix}\overline{Z}_{1,t-p}\\ \overline{Z}_{2,t-p}\\ \overline{Z}_{3,t-p}\end{bmatrix}+\begin{bmatrix}a_{1t}\\ a_{2t}\\ a_{3t}\end{bmatrix}$$

Where $\{\mathbf{Z}_t \ \mathbf{Z}_{t-1} \ \cdots \ \mathbf{Z}_{t-p}\}$ is a stable stochastic process, $\mathbf{Z}_{t-1}$, $\mathbf{Z}_{t-2}\cdots\mathbf{Z}_{t-p}$ are the stochastic processes of past time $\mathbf{Z}_t$, $\overline{\mathbf{Z}}_t=\mathbf{Z}_t-\boldsymbol{\mu}$, and $\boldsymbol{\mu}$ is the average of Z_t. Therefore, $\overline{\mathbf{Z}}_t$ is a 0-average stochastic process; Φ_1, Φ_2 and Φ_p are the autoregressive parameters of AR(p) representing the parameters to be solved in a specific stochastic series. The $\mathbf{a}_t$ in Eq. (4.4.9) can be expressed as $a_t=B_0\varepsilon_t$, where ε_t is the 0-average white noise process, and B_0 is the adjustment factor of ε_t. As ε_t is a white noise process of an arbitrary amplitude, there will its specific amplitude for AR model according to the known conditions. Therefore, ε_t must rely on B_0 to control the magnitude of its amplitude in a white noise process. In addition, the autoregressive parameters in Eq. (4.4.10) imply spatial correlation. Also, the autoregressive model features the infinite decrease of autocorrelation functions, and some of the autocorrelation functions will be lost in a finite period of time. During the generation of time series in the model, the autoregressive parameter Φ and the adjustment factor B_0 are unknown. It is necessary to determine Φ and B_0 using the known correlation functions.

Furthermore, for wind speed disturbance spectrum, the disturbance force caused by turbulence is mainly the function of wind load coefficient and disturbed wind speed. For the finite element analysis of this study, the wind attack angle is 0°, and the wind coefficient is determined from wind tunnel experiment (VCE-Vienna Consulting Engineers, 1993). For disturbed wind speed, the autoregressive model in the section above is used to convert the wind speed spectrum to time series pattern. Therefore, by converting the wind speed disturbance spectrum to time series pattern using the autoregressive model, the wind speed time history required for analysis is obtained.

For bridge analysis model, there are 2 types of nonlinear behavior in any structure, one being the geometric nonlinearity and the other being the material nonlinearity. Under general

circumstances, the materials used for the elements of a cable-stayed bridge remain in a linearly elastic range, and, therefore, only the geometric nonlinearity is considered for the nonlinear behaviors of the cable-stayed bridge. A cable-stayed bridge displays 3 types of geometrically nonlinear behavior: sagging effect of cables, beam-column effect and large displacement effect. Cables sag due to their self-weight. The size of sagging is determined by the length of cable and the magnitude of tensioning. In this study, the influence of cable sagging on the axial stiffness of cable is considered using the equivalent modulus of elasticity. In addition, the tower and bridge deck are subject to enormous axial compression because of the high tension in the stay cables. As a result, the bridge and tower are subject to axial force and bending moment at the same time, thus leading to interactions. This part is simulated using the corrected stiffness coefficient. Being a slender structure, a cable-stayed bridge often experiences larger displacement when loaded. Thus the large displacement effect must be considered in the analysis of a cable-stayed bridge. The Newton-Thomson method is used in this study for the nonlinear iterative analysis. The system equilibrium function is developed at the displaced position, and the geometric stiffness matrix is considered until the unbalanced forces converge after repeated iterations.

The autoregressive model is used to build the time histories at different wind speeds. The aerodynamic parameters (A_i^*, H_i^*) and wind force coefficient are taken from previous literature (VCE-Vienna Consulting Engineers, 1993). Also, the air density is 1.22kg/m^3, roughness length is 1.0m, damping ratio of structure is 2%, and the time history is 600 seconds with the increment of 0.01 second. First, the results from the traditional frequency domain analysis method and the time domain approach used in this study are compared. The wind speed time history is that of design wind speed at 52m/s developed using the autoregressive model. Two different methods are used for the dynamic analysis of cable-stayed bridge. **Fig. 4.14** is the time response at each of the directions obtained at the middle of the main span in the nonlinear time domain analysis. **Fig. 4.15** shows the response at different directions at the design wind speed. The maximum response of each direction is shown in **Table 4.7**. **Table 4.7** shows that the maximum response at vertical, lateral and torsional directions in the time domain analysis are at 77% span, 60% span and

mid-span of the main span with the displacements of 0.1141m, 0.0066m and 0.0354 degree, respectively. For frequency domain analysis, the maximum response at each of the 3 directions occurs at the same location, i.e. at 77% span, 60% span and mid-span of the main span, with the response of 0.1384m, 0.0070m and 0.0367 degree, respectively. Hence, **Fig. 4.14** and **Table 4.7** suggest that the result of frequency domain analysis is generally greater than that of time domain analysis, which is reasonable. If the time domain analysis result is used to calculate the difference between the both, as shown in **Table 4.7**, the error is generally within 10%. Only the difference of vertical response at 2/3 of the main span exceeds 10%.

Table 4.7 Comparison of Cable-stayed Bridge Analysis Results

Location	Item	Time domain analysis	Frequency domain analysis	Error (%)
1/2 of main span	Vertical RMS (m)	0.0781	0.0847	7.79
	Lateral RMS (m)	0.0063	0.0066	4.55
	Torsional RMS (degree)	0.0353	0.0366	3.55
2/3 of main span	Vertical RMS (m)	0.1093	0.1260	13.25
	Lateral RMS (m)	0.0065	0.0068	4.41
	Torsional RMS (degree)	0.0324	0.0338	4.14

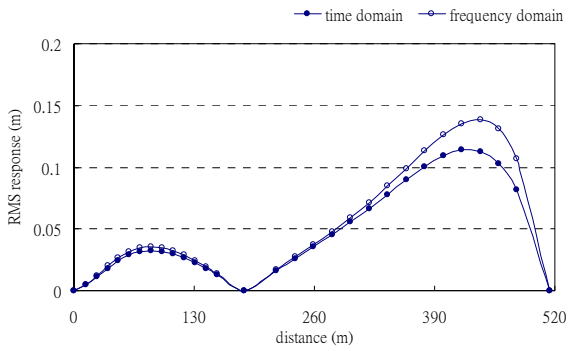

(a)

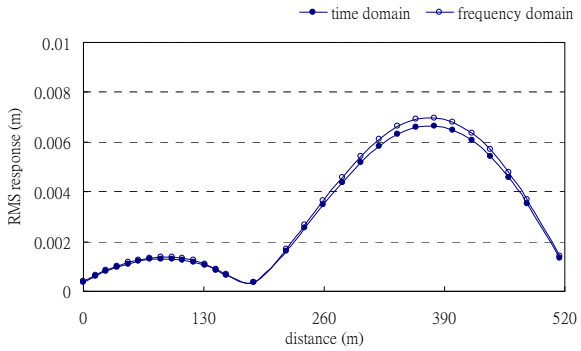

(b)

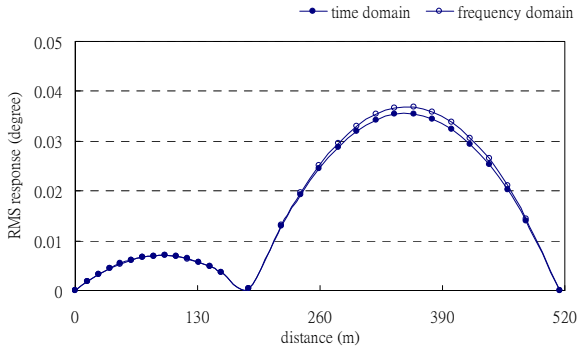

(c)

Figure 4.14 Comparison of full bridge response: (a) vertical; (b) lateral; (c) torsional (U=52m/s)

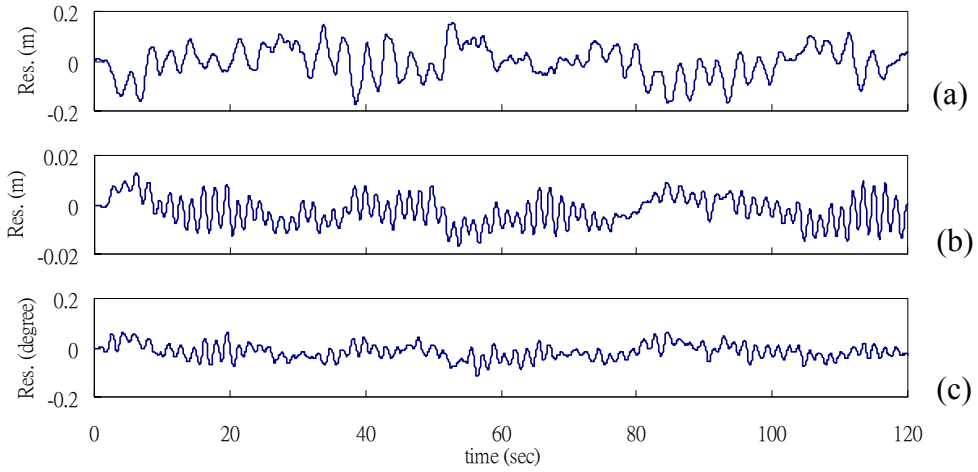

Figure 4.15 Time history of bridge deck at 1/2 of main span: (a) vertical; (b) lateral; (c) torsional (U=52m/s)

In addition to the dynamic response of the cable-stayed bridge at the design wind speed of 52m/s, the simulation is conducted at the 500-year regression wind speed of 60.8m/s and various wind speeds as well. **Fig. 4.16** shows the time-histories of the entire Bridge at the 3 directions at different wind speeds. It is learned from the figure that when wind speed increases, the response of the Bridge increases as well. However, the locations of maximum response at each of the 3

directions remain the same despite of different wind speeds. The maximum responses at vertical, lateral and torsional directions occur at 77%, 60% and 50% of main span, respectively. When the wind speed rises to the 500-year regression wind speed of 60.8m/s, the maximum responses at vertical, lateral and torsional directions are 0.1808m, 0.0100m and 0.0580 degree, respectively. **Fig. 4.17** is the changes in the maximum responses at the 3 directions in relation to different wind speeds. The figure suggests that the maximum response at each of the 3 direction increases with wind speed at 77%, 60% and 50% of main span. The responses grow in the fastest rate at vertical and torsional directions. Therefore, it is safe to say that the flutter instability of the Bridge shall be focused on these 2 directions. To predict the growth of response at the vertical direction, it will grow dramatically when wind speed is greater than 160m/s. Therefore, it is safe to say that the critical wind speed for aerodynamic instability is somewhere around this wind speed.

Nonlinear time-history analysis is conducted on the Bridge with the consideration of the geometric nonlinearity of the structure. First, the autoregressive model is used to establish the time history of wind loads, and the aerodynamic response analysis of the Bridge under wind loads is performed using the nonlinear time domain method and traditional frequency method. By summarizing the analysis result, the following conclusions are reached:

1. The use of autoregressive model for the development of wind speed time history will generate continuous time histories and help solve the problem of spatial correlation;
2. The two methods used yield relatively similar results, while the result from the traditional frequency domain method is somewhat conservative;
3. The structural responses at the 3 directions increase with wind speeds, and it is particularly true in vertical and torsional directions. Therefore, it is safe to say that the responses at vertical and torsional directions dominate the aerodynamic behaviors of a cable-stayed bridge. Further study and comparison may be necessary for wind load monitoring data.

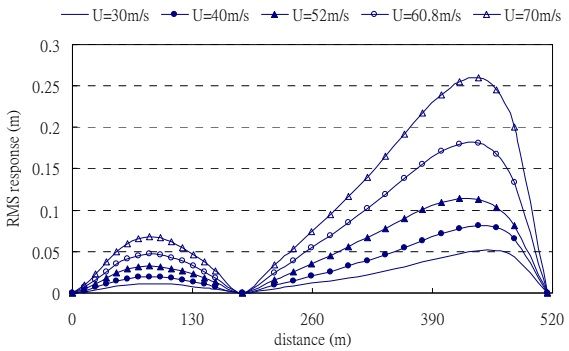

(a)

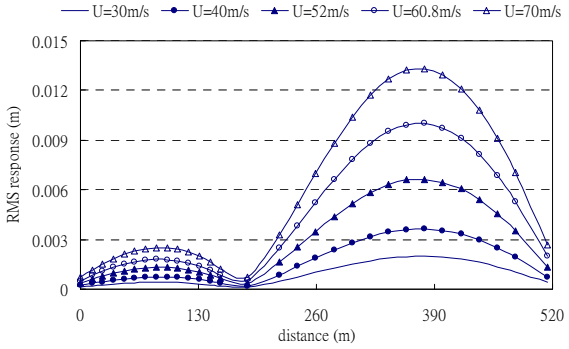

(b)

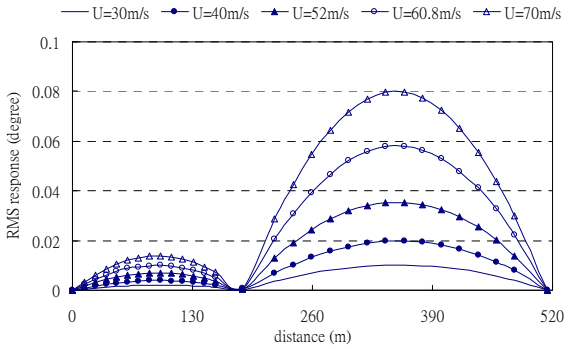

(c)

Figure 4.16 Comparison of buffeting responses at different wind speeds: (a) vertical; (b) lateral; (c) torsional

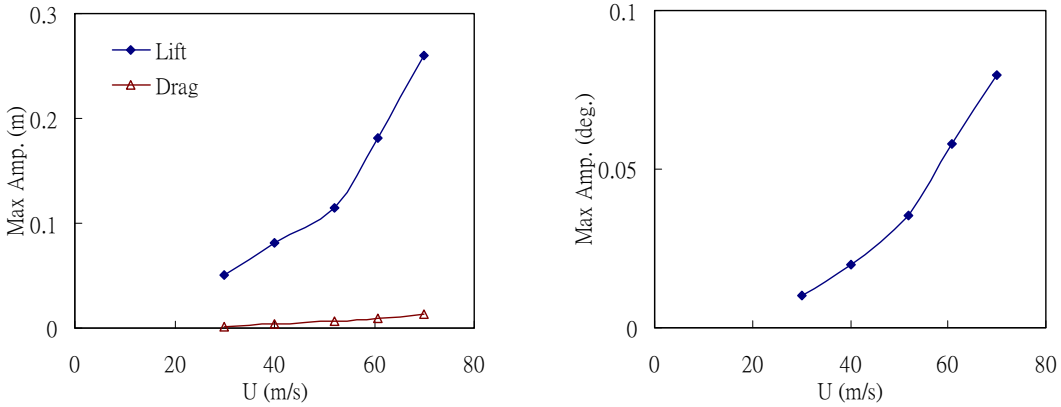

(a) (b)

Figure 4.17 Maximum responses at the 3 directions under different wind speeds vs. wind speed: (a) vertical and lateral; (b) torsional

4.5 Monitoring of Random Traffic Vibrations

A cable-stayed bridge features flexibility, light-weight and low damping. When subject to random traffic and wind loads for the long run, the bridge will display significant vibration response. This may lead to damage or failure such as fatigue in the cross section of steel structure, stay cables and other important structural elements. The long-term dynamic monitoring system is used in this study for the in-situ tests and long-term dynamic response monitoring of the Bridge. The change in dynamic responses of the Bridge subject to the peak and off-peak traffic during the day is studied. By processing the dynamic response of the cable-stayed bridge with wavelet transform, the dynamic characteristic parameters, e.g. frequency and damping ratio, are identified. The influence of vibration amplitude on the change in dynamic parameters is investigated with the Bridge subject to traffic. The result of this study suggests that the change of natural frequencies of the Bridge is not distinctive when the Bridge is under different vibration amplitudes. However, the change is more obvious for the modal damping ratio.

For the processing of the data obtained from the dynamic tests, the vibration signals of the Bridge are converted to free attenuation vibration signals using random decrement, and the dynamic characteristics of the Bridge are identified with the Meyer wavelet function as the basis function of CWT. The first 5 modal natural frequencies and damping ratios identified at each of the 3 directions are shown in **Table 4.8** and **Table 4.9**. The identification result of vertical direction shown in **Table 4.8** indicates that the first natural frequency in vertical direction is 0.284Hz with a damping ratio of 2.9%, whereas the same frequency obtained from the monitoring data is 0.284Hz, both of which are very close, and the same can be said for other modes. The vibration test result shown in **Table 4.9** indicates that the first lateral frequency is 0.643Hz with a damping ratio of 3.3%, while the same frequency obtained from the monitoring data is 0.686Hz. This time, the identification result from the monitoring data is slightly higher, but the natural

frequencies identified for other modes are quite close.

For tests at the torsional direction, the vibration test is not performed at this direction due to lack of proper instrument. Only the monitoring system is used for measurement. The result obtained from CWT is shown in **Table 4.10**. No further analysis is performed at the torsional direction.

The monitoring study on the traffic of the Bridge was carried out for 18 months from June 2007 to the end of 2007. To learn more about the influence of normal traffic to the Bridge, the monitoring data were selected from one day between the period of Aug 22 2006 ~ Feb 13 2007. As there was no major earthquake or typhoon at Kaohsiung and Pingtung during this period, the monitoring data do not contain any influence of earthquake or typhoon. The monitoring data was sampled once every 10 minutes, and therefore, the root-mean-square (RMS) of the vibration response was selected as the magnitude of vibration. As result, 144 RMS values of vibration magnitude were obtained during a 24-hour observation period, as shown in **Fig. 4.18**.

Table 4.8 Dynamic Characteristics of the Bridge at the Vertical Direction

Mode	Ambient Test		Structural monitoring	
	f (Hz)	ξ (%)	f (Hz)	ξ (%)
1	0.284	2.9	0.284	2.8
2	0.574	3.7	0.533	3.8
3	0.92	4.4	0.97	4.6
4	1.54	3.9	1.50	3.6
5	1.81	3.0	1.88	3.3

Table 4.9 Dynamic Characteristics of the Bridge at the Lateral Direction

Mode	Ambient Test		Structural Monitoring	
	f (Hz)	ξ (%)	f (Hz)	ξ (%)
1	0.643	3.3	0.686	2.0
2	1.64	2.9	1.65	3.3
3	2.17	3.2	2.15	2.9
4	2.51	2.5	2.53	3.0
5	3.13	3.9	3.11	3.6

Table 4.10 Dynamic Characteristics of the Bridge at the Torsional Direction

Mode	Structural Monitoring	
	f (Hz)	ξ(%)
1	0.754	1.84

2	1.46	1.09
3	2.18	1.29
4	2.91	1.82
5	3.68	1.69

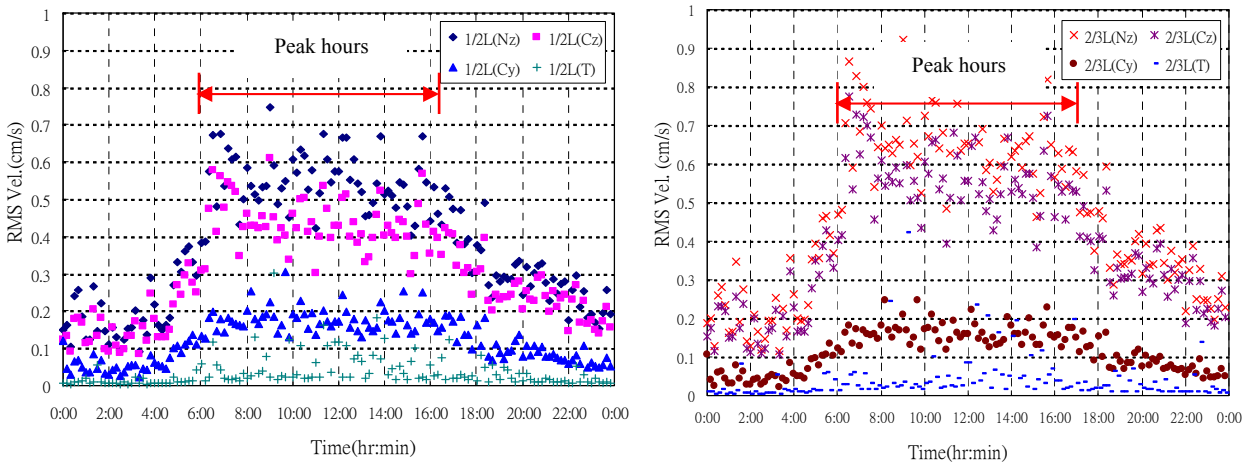

(a) (b)

Figure 4.18 Changes of Vertical Vibration Magnitude of the Bridge over Time: (a). at 1/2 span; and (b). at 2/3 span

The Bridge is one of the thresholds for daily north and southbound traffic in Kaohsiung and Pingtung. It is not difficult to identify in the 24-hour observation period that the peak hours are from 6:00 a.m. to 6:00 p.m., during which the vibration magnitude increases dramatically, whereas the off-peak hours are from 6:00 p.m. to 6:00 a.m., during which the vibration decreases significantly. Take the vertical vibration response at the vertical direction at 1/2 span as an example. The average peak response reaches as high as 0.7~0.8cm/s; while the response to off-peak traffic is 0.2~0.3cm/s. Therefore, the vibration of the Bridge is 2.5~3.5 times greater during the peak hours than during the off-peak hours. This result indicates that the background vibration of the Bridge is approximately 0.2cm/s when the Bridge is subject to ambient vibration.

In addition in section 4.3, the influence of traffic amplitude to the dynamic characteristic parameters, the data of peak hours from 7:00 to 9:00 a.m. are selected to investigate the influence of the bridge vibration magnitude to the dynamic characteristic parameters. The RMS is calculated for the vibrations taken every 10 minutes, and the CWT is used to identify the dynamic

characteristics of the Bridge, including natural frequencies and damping ratio. The analysis results are shown in **Fig. 4.19** and **Fig. 4.20**.

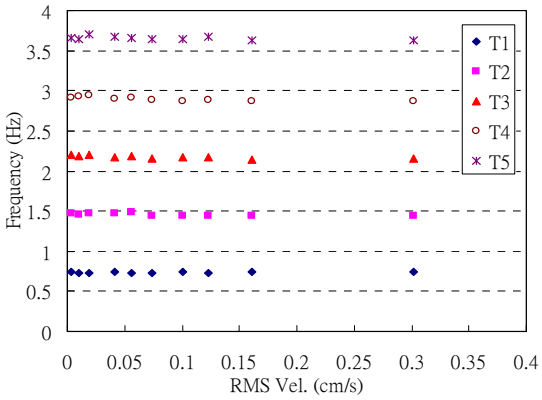

Figure 4.19 Change of Frequency of the Bridge at Torsional Direction with Amplitude

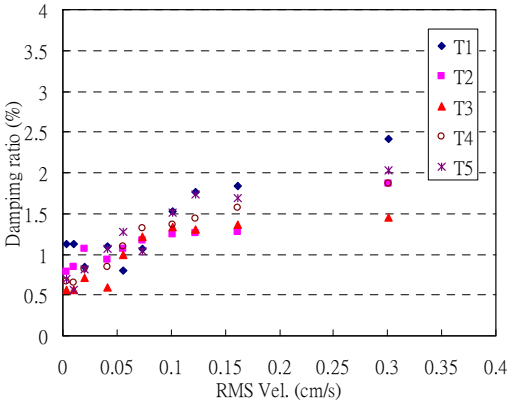

Figure 4.20 Change of Modal Damping Ratio of the Bridge at Torsional Direction with Amplitude

Fig. 4.19 shows that the RMS of traffic vibration falls between 0.08 and 0.72cm/s, and the first natural frequency at vertical direction ranges from 0.272 to 0.282Hz. Hence, the vibration magnitude of the Bridge has little influence to the first natural frequency at vertical direction. Also shown in **Fig. 4.20**, the first modal damping ratio identified ranges from 1.63 to 3.43% within the same range of vibration magnitude, and the damping ration increases with the vibration magnitude, indicating that the modal damping ratio is very sensitive to bridge vibration, whereas the same cannot be said for the frequencies. Therefore, if the traffic-induced vibration is used as benchmark and the change of modal damping ratio as the parameter of damage diagnosis, the change of damage in the cable-stayed bridge can be determined after a long period of monitoring.

In-situ vibration tests and monitoring are conducted for the Bridge and CWT is introduced for modal identification. It is possible to identify the dynamic characteristic parameters of the Bridge from the data of vibration test and monitoring. For model building, the cable-stayed bridge consists of various special elements and is supported in a different manner from other bridges, so it requires careful attention in simulating the cable elements and boundary condition at supports. For system identification, CWT is used practically for the processing of data obtained from in-situ tests and monitoring, and the dynamic characteristic parameters of the Bridge are identified and the data of the first 5 modes at the 3 directions are determined. The results obtained are quite consistent with those determined by the analysis of the model built. The MAC values of modal shape are all greater than 0.9, indicating that not only the data provided by the monitoring system is correct, but also the analysis model built for this study is a reasonable one.

Also, the long-term traffic dynamic responses of the Bridge are monitored and the traffic-induced vibrations are used to investigate the changes o dynamic characteristics of the Bridge. The response of the Bridge is analyzed under normal traffic. For the dynamic characteristic parameters of the Bridge, the change of natural frequencies is not significant under different vibration magnitudes. However, the modal damping ratio displays more significant change. This result helps build a health diagnosis method with the traffic vibrations as the measurement basis and the damping ratio the damage parameter for the safety monitoring of the Bridge in the future.

5. Disaster and emergency response plan

5.1 Bridge Safety Assessment

On the completion of the monitoring system, it was first used for the assessment of the Bridge's health using the monitoring data. The analysis of monitoring data, interpretation of the results, the assessment of current structural health, the management of monitoring data and function reports were performed. The assessment process for the structural health is shown in **Fig. 5.1**.

The assessment of existing performance of the Bridge is based on the monitoring data with the assistance of design data and in-situ inspections. The response signal processing and analysis process for wind and seismic loads are shown in **Fig. 5.2 and Fig. 5.3**, respectively. It is now possible to perform assessment on important parameters on the vibration response of the Bridge when it is subject to changes of wind speed and direction, earthquakes and traffic loads.

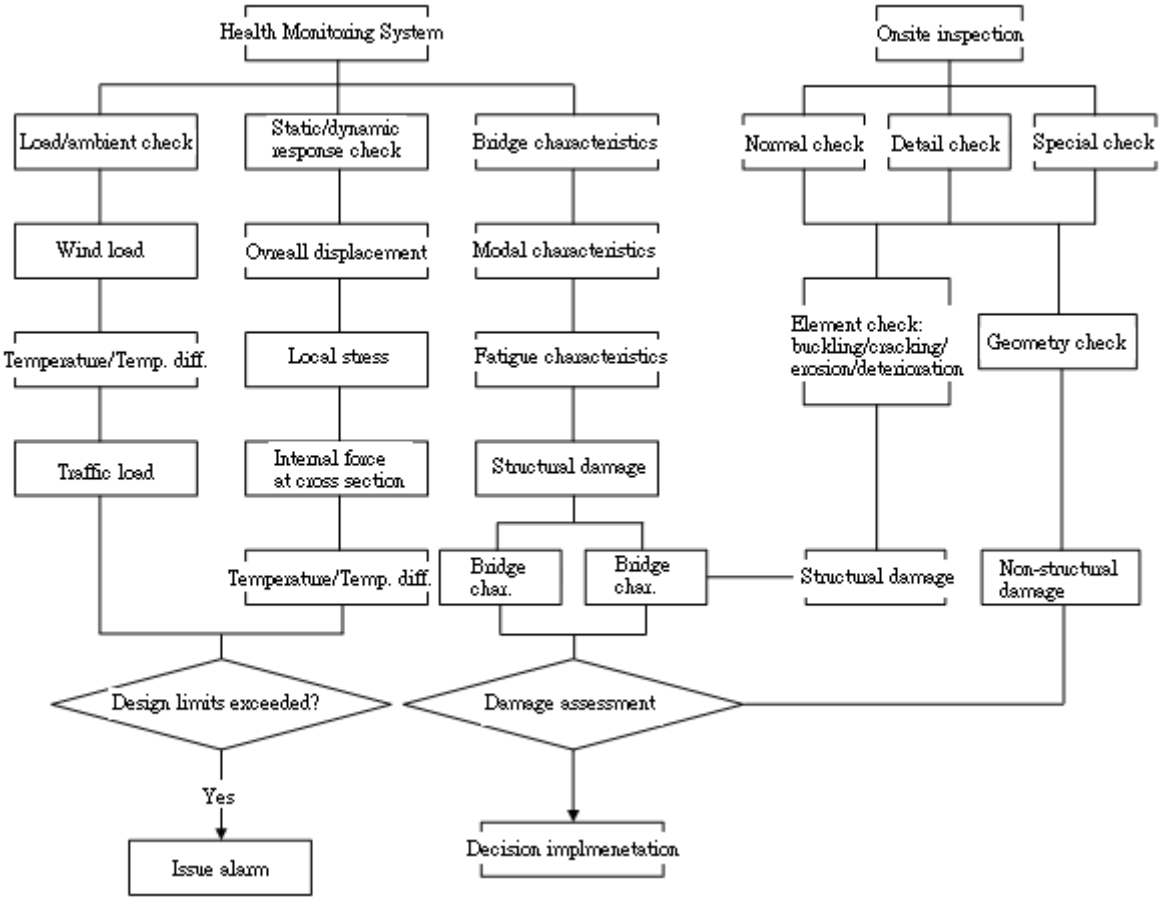

Figure 5.1 Flow Chart for Structural Health Assessment Process

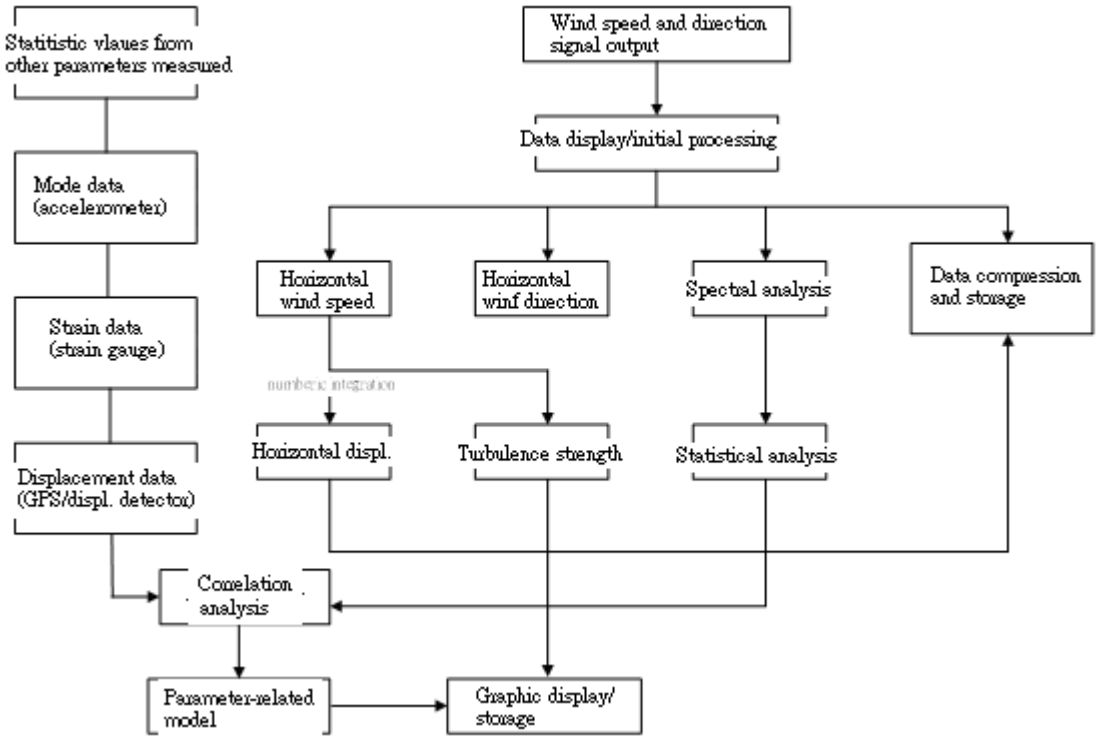

Figure 5.2 Flow Chart for the Analysis of Wind Speed and Direction Signal Processing

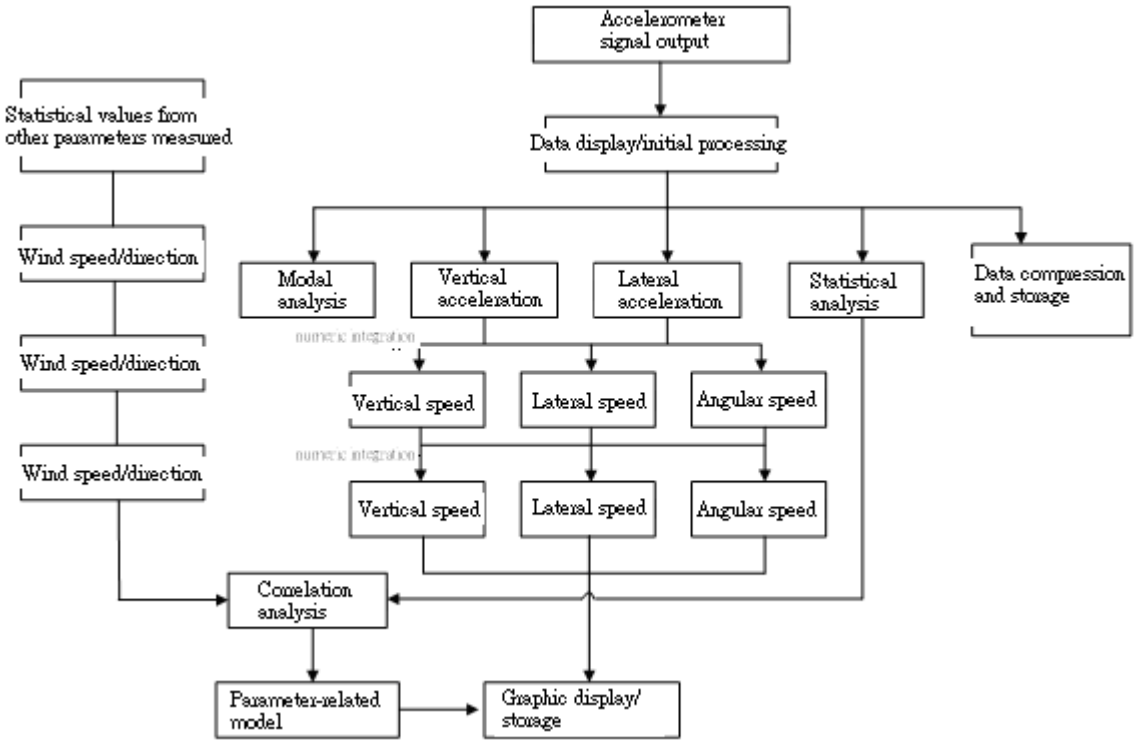

Figure 5.3 Flow Chart for Vibration Signal Processing

5.2 Establishment of Bridge Alarm

After the assessment, the bridge monitoring data can be used for the following applications:

1. To provide the reference basis for the establishment of alarm system; i.e. how to establish effective alarm thresholds;
2. To revise the parameters of the original design, to make the analysis model reflect the real behaviors more so it can be used as the basis of the structure aging and deterioration evaluation; and
3. To help develop alarm levels and real-time response strategies.

The alarm system works by summarizing the data from the monitoring system into a database for analysis and evaluation, and an assessment system of structural danger level is developed to provide the management system the basis on which the crisis management and maintenance are performed. What is the most important aspect about the assessment system is the development of alarm criteria. The alarm thresholds established include alarm values and action values.

1. Alarm value: it refers to the upper limit of the readings registered in the monitoring instrument under the operations of the structure. When the monitoring value exceeds the alarm value, it generally indicates that an unusual condition occurs to the function of instrument or the structure unless it is a misjudgment of instrument or other special causes. However, the danger level is not reached.
2. Action value: it refers to the maximum tolerance of a structure. When the monitoring value exceeds the action value, it indicates that the structure is in a critical condition, and response actions must be taken.

Also, for the setting of alarm and action values, the alarm value for a structure is developed based on the evaluation of changes in monitoring parameters, regular changes in the time-history curves plotted from the monitoring value, and the changes in the characteristics, trends and causal correlation. In general, there are two evaluation methods, one being qualitative and the other quantitative. The two can be used independently or together depending on structure types, timing and practical needs. The qualitative evaluation works to identify and evaluate based on the stability, correlation, reasonability, mutability and symmetry of the time-history curves plotted using monitoring data. On the other hand, the quantitative analysis works to evaluate whether a

structure is working normally, not working well or in a critical situation using the values determined from the monitoring data theoretically, statistically or empirically.

The principles and method of alarm value development are:

1. To estimate the range of threshold variance based on the upper and lower limits of long-term monitoring data to serve as the reference of alarm and action values;
2. To calculate the threshold for monitoring factors using structure engineering analysis in order to provide the reference of alarm and action values; and
3. To determine the final alarm and action values based on the analysis data mentioned above after the instruments and system are set up and the two analyses mentioned above start.

Cable-stayed bridge is a complicated structure with multiple alarm values of, for example, displacement, stress, strain, dynamic acceleration, wind speed and direction, and cable tensioning. These many alarm values have direct influence to the safety of a bridge. However, these values may or may occur all at the same time, and there is possibly difference in levels. Therefore, these alarm values must be considered together. The principle of multiple monitoring is adopted to develop a so-called alarm index (AI) for the all-round consideration of the overall critical status of the Bridge.

5.3 Bridge Alarm Levels and Emergency Response Actions

The items monitored by the alarm system include tilting and displacement of the tower and piers, vibration of bridge, wind vibration, traffic and seismic response, cable vibration and loss of tensioning, wind effects at the bridge site and settlement of piers. The monitoring data are analyzed and interpreted at the monitoring center, and relayed to the maintenance supplier or construction supervisor on a fixed schedule or immediately for the initiation of alarming actions. The alarm is designed as an alarm system. When the Bridge is subject to an unexpected earthquake or high wind, the monitoring center has to analyze and check the behaviors of the structure immediately. If the Bridge is loaded, the alarm system will sound an alarm immediately when the dynamic behavior reaches the alarm value, and the alarm is relayed to the maintenance

operator to initiate emergency response, ensuring the safety of traffic and drivers.

The Bridge is located on a national transportation artery. As a result, proper traffic control and safety have great influence, for which close monitoring is required. 5 levels are developed based on seriousness, and allow the bridge users, supervisor, consultants and monitoring operator to sound the alarm of different level. The alarm levels, conditions and the emergency response actions for individual departments are shown in **Table 5.1**. More reliable array of alarm and action values may be developed based on the analysis of the monitoring data in the future.

Table 5.1 Alarm Level Criteria and Emergency Response Actions for Individual Department

Level	Condition	User	Manager	Consultant	Monitoring Dept.
Level 1 (Action value is reached)	1. α% of the seismic load registered reaches or exceeds the design seismic load. 2. α% of the wind load reaches the design wind load. 3. γ% of data registered in the monitoring instrument reaches the design value.	Red alarm to users	Bridge closure is initiated and bridge management department arrives on site immediately along with consultants, instrument operators and experts for damage evaluation and response actions.	On-site presence required	Check instruments immediately on site.
Level 2 (Alarm value is reached)	1. The seismic load reaches or is somewhat lower than the design seismic load. 2. The wind load reaches or is somewhat lower than the design wind load. 3. λ% of data registered in the monitoring instrument reaches the design value.	Yellow alarm to users	Safety inspection is required within a given deadline.	On-site presence required afterwards	Check instruments on site afterwards.
Level 3	Torrential rain, typhoon, earthquake and other special conditions		The bridge management dept. is informed.	Consultant informed	Increase monitoring frequency
Level 4	Any result occurs that exceeds regular monitoring values.		The bridge management dept. is informed.	Consultant informed	Increase monitoring frequency

Level	Condition	User	Manager	Consultant	Monitoring Dept.
Level 5	Normal (general condition)）				Regular data capturing

Note: α, γ and λ shown in the table must be determined for the structure system after monitoring and detailed analysis for a long period of time.

6. Conclusion

The Kao Ping Hsi Cable-Stayed Bridge is the longest cable-stayed bridge in Taiwan. It features a slender, light-weight and flexible structure. As a result, it is important to monitoring not only seismic activities, but also wind loads to which the Bridge is more sensitive. The Bridge has been in service for more than a decade, and it is a forward-looking conduct to establish a bridge health monitoring system to ensure its safety. By monitoring the overall safety of structure in terms of seismic reactions, wind resisting behaviors and cable vibrations during the Bridge's operation and the comfort of driving in the long run, more alarm information will be collected for the reference basis for the management and maintenance of safety in event of earthquakes, wind vibrations and heavy traffic. Thus, the first part of the study is focused on the introduction to the skills for in-situ vibration monitoring and measurement to gather basic characteristics of the Bridge, which are used for the basis of comparison with the health monitoring performed by the BHMS; the second part is the introduction to the layout of the complete BHMS and the design principles for its functions for the basis of bridge characteristics monitoring and the evaluation of bridge safety in the future. The following are the conclusions:

1. A thorough design is conducted for the monitoring system. The establishment is separated 2 in stages. The stage one plan is the "system establishment and data collection," and the stage two plan is the "functional performance and practical implementation," both of which are advance practices.
2. The stage one "system establishment and data collection" aims to establish the system structure and collect first data. The works include the installation of basic monitoring instrumentation

required in the contract, system establishment, data recording, monitoring and preliminary data collection.

3. In stage two "functional performance and practical implementation," the aim is to combine both traffic control and the monitoring system to initiate the announcement of alarm for danger and bridge closing for the actions and purpose of bridge safety monitoring. The alarm values are established with the concept of multiple monitoring as the basis for traffic control and to increase the reliability of alarm announcement. Monitoring spots and items are increased based on safety control and practical functioning need for the goal of monitoring, control and safety.
4. While the monitoring system structure is developed, it is necessary to leave some room for expansion of instruments and wiring. It helps prevent maintenance costs and the compatibility concern in the integration of traffic control and the monitoring system, and avoids the complexity in the system operations and data collection in the future.

The benchmarks established for the comparison of the characteristics of the Bridge for long-term monitoring preparation include:

1. Vibration test and system identification: to establish a reasonable finite element analysis model for seismic and wind loading analysis.
2. Cable tensioning measurement and analysis: to establish the clear picture of the tensioning on all cables for the behavioral analysis of the wind and rain vibrations of the Bridge.
3. Aerodynamic stability analysis: to carry out the aerodynamic stability analysis of the entire Bridge.
4. Influence of traffic effects on bridge vibrations.

In addition, the Bridge is one on national freeway. An alarm can be issued only when the damage is determined very accurately when the Bridge is loaded. As a result, all the monitoring indicators must be collected and studied to reach the demand for multiple monitoring indicators and to arrive at the best judgment. It is hoped to modify the alarm indicators to best fit the maintenance management requirements with the long-term monitoring results in the future, and, as

the demand for the safety maintenance and management of the Bridge is fulfilled, the monitoring and maintenance works of the Bridge will serve as an example for the bridge safety monitoring of the country.

References

[1] Yang, Yung-Ping and Chen, Cheng-Hwa (1995[a]), "Review of cable-stayed bridge theory development – Part 2: 1880s to 1940s," *Structure Engineering*, Taipei Taiwan, Vol. 10, Ed. 3, 9. 45-62.

[2] Yang, Yung-Ping and Chen, Cheng-Hwa (1995[b]), "Review of cable-stayed bridge theory development – Part 3: 1880s to 1940s," *Structure Engineering*, Taipei Taiwan, Vol. 10, Ed. 4, p. 65-88.

[3] Chen, Cheng-Hwa and Weng, Cheng-Yu (2007), "Study on the statistic relation between normal dynamic response and alarm values for cable-stayed bridges," proceedings of the 16th Southern Taiwan Statistics Conference, Kaohsiung, National University of Kaohsiung, June, 22-23, paper No. 12.

[4] Taiwan Area National Expressway Engineering Bureau, Ministry of the Interior (2002), "Kao Ping Hsi Cable-Stayed Bridge," Taipei, Taiwan.

[5] Chen, Cheng-Hwa, Ouyang, Chen, Huang, Ming-Chih and Chen, Tang-Cheng (2005[a]), "Measurement and analysis of the tensioning force in the stay cables of cable-stayed bridge under traffic," proceedings of the 29th National Mechanics Meeting, National Tsing Hua University, D013.

[6] Chang, Yi-Hsian (2001), "Cable tensioning monitoring techniques for cable-stayed bridges," master thesis for Graduate Institute of Civil Engineering, National Cheng Kung University, instructor: Prof. Fang, Yi-Kuang.

[7] Chen, Cheng-Hwa, Tang, Hui-Hsiung and Ouyang, Chen (2005[b]), Measurement and analysis of stay cable tensioning in a cable-stayed bridge – steel arch cable-stayed bridge over Maoluo River," *Structure Engineering*, Taipei Taiwan, Vol. 12, Ed. 3, p. 61-72.

[8] Siegert, D., and Brevet, P., (2006) “Fatigue of stay cables inside end fittings high frequencies of wind induced vibrations,” Laboratoire Central des Ponts et Chaussées, France.

[9] Zui, H., Shinke, T., and Namita, Y., (1996), “Practical formulas for estimation of cable tension by vibration method,” *Journal of Engineering Mechanics*, 122(6), 651-656.

[10] Takahashi, K., (1991) “Dynamic stability of cables subjected to an axial periodic load,” *Journal of Sound and Vibration*, **144**, 323-330.

[11] Ren, W. X., Peng, X. L., and Lin, Y. Q., (2005) “Experimental and analytical studies on dynamic characteristics of large span cable-stayed bridge,” *Engineering Structures*, **27**, 535-548.